Gas Adsorption in Volumetric System

By

Metin BECER

**A Dissertation Submitted to the
Graduate School in Partial Fulfillment of the
Requirements for the Degree of**

MASTER OF SCIENCE

**Department: Chemical Engineering
Major: Chemical Engineering**

**İzmir Institute of Technology
İzmir, Turkey**

May, 2003

We approve the thesis of **Metin BECER**

Date of Signature

..... **24.05.2003**

Asst. Prof. S. Fehime ÖZKAN
Supervisor

Department of Chemical Engineering

..... **24.05.2003**

Prof. Dr. Devrim BALKÖSE
Co-Supervisor

Department of Chemical Engineering

..... **24.05.2003**

Prof. Dr. A. Semra ÜLKÜ
Co-Supervisor

Department of Chemical Engineering

..... **24.05.2003**

Prof. Dr. Gönül GÜNDÜZ

Department of Chemical Engineering

..... **24.05.2003**

Asst. Prof. Erol ŞEKER
Department of Chemical Engineering

..... **24.05.2003**

Prof. Dr. Devrim BALKÖSE
Head of Department

ACKNOWLEDGEMENTS

I would like to express my intimate gratitude to my advisor, Asst. Prof. Fehime Özkan, for her guidance and support throughout this project. I am also grateful to Prof. Dr. Devrim Balköse, Prof. Dr. Semra Ülkü and Prof. Dr. Gönül Gündüz for their valuable suggestions. I also would like give my special thanks to Asst. Prof. Erol Şeker for his valuable recommendations during the study.

I would like to thank all of the experts in the Chemical Engineering Department of İzmir Institute of Technology, laboratory technicians and especially to the experts in the CMS (Center for Materials Research) for their contributions to the characterization studies presented in this study.

I would like to appreciate deeply to my roommates, Mehmet Gönen, Sevdiye Atakul, Hacer Yenal and Yılmaz Yürekli for their friendships, supports and encouragements.

Finally, my thanks go to my family for their help and supports.

ABSTRACT

In this study, nitrogen adsorption on natural zeolitic tuff from Gördes, (Fındıcak) region and on its acid treated forms was studied. The natural zeolite, identified as clinoptilolite, has been treated with HCl, H_2SO_4, HNO_3, and H_3PO_4 solutions at several concentrations to obtain the acid treated forms. Structural modifications arising from the acid treatments were determined by the techniques, namely XRD, FTIR, ICP, EDX, SEM, DTA, TGA, and microcalorimeter. Adsorption characteristics of zeolites, such as external and total surface areas, micropore volumes and pore size distributions were compared.

Acid treatment of natural zeolite showed that as the acid concentrations were increased, more cations were removed from the structure, changing the Si/Al ratios from 4.04 (original zeolite) to 5.35 with H_2SO_4, to 6.39 with HNO_3, to 10.8 with HCl and to 5.01 with H_3PO_4 treatments respectively. With acid treatment, the maximum nitrogen adsorption capacity at P/P_o = 0.89 of natural zeolite (0.015 cm^3/g) was increased to 0.089, 0.090, 0.086, and 0.050 cm^3/g for HCl, HNO_3, H_2SO_4 and H_3PO_4 treatments respectively. Nitrogen adsorption capacities of the zeolites increased with increasing Si/Al ratios, but further increase in concentrations caused to decrease the adsorption capacity for HCl and HNO_3 treatments. HCl behaved in a different way that, dilute (1M) and highly concentrated (10 M) solutions has effect on the framework structure much more than the middle range concentrations (3 M and 5 M HCl) decreasing the nitrogen adsorption after Si/Al = 8.4 (5 M HCl).

Dubinin-Raduskhevich model was used to determine the volume accessible to nitrogen (limiting micropore volume). It increased with increasing Si/Al ratios, but further increase in concentrations caused to decrease in microporous structure. The highest limiting micropore volumes (0.078 and 0.082 cm^3/g), and Langmuir surface areas (213 and 226 m^2/g) were obtained with the 5 M HCl and 2 M HNO_3 treated samples respectively without any noticable loss in crystallinity.

ÖZ

Bu çalışmada, Gördes, Fındıcak bölgesinden elde edilen doğal zeolitik tüfün ve bu tüfün asit ile işlem görmüş hallerinin azot adsorpsiyonu çalışılmıştır. Klinoptilolit olarak tanımlanan doğal zeolit, çeşitli konsantrasyonlarda HCl, H_2SO_4, HNO_3 ve H_3PO_4 çözeltileri ile işleme tabi tutulmuştur. İşlemler sonucunda meydana gelen yapısal değişimler çeşitli karakterizasyon yöntemleri kullanılarak saptanmıştır. Bu karakterizasyon yöntemleri, X-ışınımı kırınımı, FTIR, ICP, EDX, SEM, DTA, TGA, ve mikrokalorimetredir. Zeolitlerin adsorpsiyon özellikleri, dış ve toplam yüzey alanları, mikrogözenek hacimleri ve gözenek boyu dağılımları karşılaştırmalı olarak incelenmiştir.

Asit işlemi sonucunda asit konsantrasyonunun artması ile birlikte yapıdan daha fazla katyonun uzaklaştığı ve bunun da Si/Al oranını H_2SO_4 kullanımı ile orjinal zeolitte bulunan 4.04 değerinden 5.35'e, HNO_3 kullanımı ile 6.39'a, HCl kullanımı ile 10.8'e, ve H_3PO_4 ile de 5.01'e değiştirdiği görülmüştür. Asit işlemi ile $P/P_o = 0.89$' daki maksimum azot adsorpsiyon kapasitesi, orijinal zeolitte bulunan 0.015 cm^3/g değerinden, HCl ile 0.089 cm^3/g, HNO_3 ile 0.090 cm^3/g, H_2SO_4 ile 0.086 cm^3/g, ve H_3PO_4 ile 0.050 cm^3/g'a yükselmiştir. Zeolitlerin azot adsorplama kapasiteleri Si/Al oranının artması ile birlikte artış göstermiş, fakat HCl ve HNO_3 kullanımında konsantrasyonun daha da artması ile birlikte düşme göstermiştir. HCl değişik bir davranış sergileyerek, düşük (1 M) ve yüksek konsantrasyonlarının (10 M), zeolitin iç yapısına, orta şiddet (3M ve 5M HCl) konsantrasyonlarına oranla daha fazla etkili olduğu ve azot alım kapasitesinin 5 M HCl ile işlem görmüş (Si/Al=8.4) örnekten sonra azaldığı bulunmuştur.

Azotun ulaşabileceği hacmin (sınırlı mikrogözenek hacim) belirlenmesi için Dubinin-Raduskhevich modeli uygulanmıştır. Si/Al oranının artması ile birlikte artış göstermiş, fakat yüksek konsantrasyonlardaki asit çözeltileri mikrogözenek yapının bozunmasına neden olmuştur. Kristal yapılarında önemli bir azalma gözlenmeden, en yüksek sınırlı mikrogözenek hacimler (0.078 ve 0.082 cm^3/g) ve Langmuir yüzey alanları (213 ve 226 m^2/g) sırası ile 5 M HCl ve 2 M HNO_3 ile işlem görmüş zeolitlerde elde edilmiştir.

TABLE OF CONTENTS

LIST OF FIGURES

LIST OF TABLES

Page

CHAPTER 1

INTRODUCTION

There has been a significant interest in recent years (Triebe and Tezel, 1995, Huesca et al, 1999, Rege et al, 2000, Armenta et al, 2001, Armenta and Jimenez, 2001, Yaşyerli et al, 2002) to prepare adsorbents for gas separation / purification by adsorption. Adsorption is of great technological importance and as well as its usage in industry for separating and purifying several gases and liquids, it is also used as a characterization tool for the texture of species

Among the other adsorbents used in industry for gas separation / purification, there exists a growing interest for zeolites. Zeolites are porous, crystalline, hydrated aluminosilicates of alkali and alkaline earth cations that posses a three-dimensional structure. The zeolite framework consists of an assemblage of SiO_4 and AlO_4 tetrahedra joined together in various regular arrangements through shared oxygen atoms to form an open crystal structure containing pores of molecular dimensions into which guest molecules can penetrate. The negative charge created by the substitution of an AlO_4 tetrahedron for a SiO_4 tetrahedron is balanced by exchangeable cations (e.g., Na^+, K^+, Ca^{2+}, Mg^{2+}), which are located in large structural channels and cavities throughout the structure (Armenta et al, 2001).

Clinoptilolite, which is a member of the heulandite group, is the most abundant of the natural zeolites. Compositions and purity vary widely among the many deposits found throughout the world (Ackley and Yang, 1991). Such deposits are commercially important because clinoptilolite tuffs are often rather pure and can be mined with simple techniques. Western Anatolia, in Turkey, has very large clinoptilolite reserves. Gördes and Bigadiç are the most known regions as clinoptilolite reserves (Yaşyerli et al, 2002). Bigadiç region has one of the most clinoptilolite occurrence in Turkey with an estimated reserve of 2 billion tons (Abusafa and Yücel, 2002).

Due to the ion-exchange and adsorption properties of the clinoptilolite, it has been applied to gas and radioactive wastewater cleaning, gas separation, gas cleaning, nutrification of animals, soil fertilizing purposes and also catalytic reactions (Malherbe, 2001, Armenta et al, 2001, Armbruster, 2001, Ghobarkar et al, 2000, Ackley and Yang, 1991, Yaşyerli et al, 2002, Triebe and Tezel, 1995).

Natural zeolites occur in huge masses and are cheaper than the sol-gel derived synthetic ones, but there is always the problem of impurities, which block the channel system (Ghobarkar et al, 2000). One of the procedures that is commonly used in order to remove the impurities and alter the adsorption properties of natural zeolites by dealuminating the structure, is leaching them with mineral acids. The acid treatment exchanges cations of the zeolite with H^+ and causes the dealumination of the structure, increasing the micropore volume and area of the zeolite, which result with enhanced adsorption capacities. Furthermore, dealumination can cause the partial or total destruction of the zeolite framework leading to a modification in zeolite morphology, by destruction of channel-blocking impurities and the development of the secondary porosity (Malherbe, 2001). Type and concentration of the acid, temperature and treatment time are all important parameters in the acid treatment studies. Up to now many scientists have dealt with these parameters (Pozas et al, 1996, Malherbe, 2001, Giudici et al, 2000, Notario et al, 1995).

This study aims to characterize the natural zeolitic tuff from Manisa, Gördes, Fındıcak region (Turkey) and its acid modified (HCl, HNO_3, H_2SO_4, H_3PO_4) forms in order to select and therefore suggest the best modified zeolite to be used further in any probable adsorption studies based on mainly nitrogen adsorption since acid treatment of natural zeolites result in enhanced adsorption capacities for molecules that are nonpolar or with small quadrupole moments such as nitrogen (Malherbe, 2001).

CHAPTER 2
ADSORPTION

Adsorption occurs whenever a solid surface is exposed to a gas or liquid, it is defined as the enrichment of material or increase in the density of the fluid in the vicinity of an interface. Adsorbate is the substance in the adsorbed state and adsorbent is the solid material on which adsorption occurs (Gregg and Sing, 1982). The overall effect of adsorption is dependent on the extent of the interfacial area. Therefore, all industrial adsorbents have large specific surface areas and are highly porous or composed of very fine particles. Porous solid is defined as a solid with cavities or channels, which are deeper than they are wide. Porosity is usually defined as the ratio of the volume of pores and voids to the volume occupied by the solid. The pore volume is usually regarded as the volume of open pores (cavity or channel with access to the surface) but it may include the closed pores (cavity not connected to the surface). Pores are classified into three classes according to their internal pore widths (diameter of cylindrical pore or distance between opposite walls of slit).

- Micropore : Pore of internal width < 20 Å
- Mesopore: Pore of internal width between 20- 500 Å
- Macropore: Pore of internal width > 500 Å

The basis for the pore classifications presented above is that each size range corresponds to different adsorption effects, as observed in an adsorption isotherm. The interaction potential in micropores is much greater than that in larger pores due to the closeness of the pore walls, resulting in an enhanced adsorption potential.

Surface area is the extent of total surface area as determined by a given method under stated conditions. Area of surface outside pores is called as

external surface area and the area of pore walls is called as the internal surface area. In many cases the internal surface area is much larger than the external surface area (Rouquerol et al, 1999).

Ancient Egyptians, Greeks and Romans were aware of the usage of some materials such as clay, sand and wood charcoal as adsorbents to be used in the desalination of water, the clarification of fat and oil and the treatment of many diseases (Rouquerol et al, 1999). But Scheele performed the earliest quantitative studies in 1773. Therefore the time of the discovery of the phenomenon of *adsorption* may be regarded as over two centuries ago. The uptake of gases by charcoal was studied by C. W. Scheele in 1773 and by F. Fontana in 1777. In their studies, the phenomenon of increasing in concentration of gas molecules in neighboring solid surfaces was noted. It was soon realized that the volume taken up differs one another if any other charcoal or any other gas is used. The dependence of the solid efficiency to the exposed surface area of the solid was then realized. The term *adsorption* was first used by Kayser in 1881 to explain the condensation of gases on free surfaces and the first attempts to relate the amount of gas adsorbed to the pressure was done by the same scientist at that year (Gregg and Sing, 1982).

Adsorption in zeolites was initially reported by Grandjean in 1910 and later studied by Weigel and Steinhof in 1925, McBain in 1926, Sameshina in 1929 and Tiselius in 1934. The notion of zeolites as " molecular sieves " was introduced by McBain in 1932 to describe the size selectivity of zeolites during molecular adsorption (Malherbe, 2000).

Adsorption is of great technological importance. Some adsorbents are used on a large scale as desiccants, catalysts or catalyst supports; others are used for the separation of gases, the purification of liquids, pollution control or for respiratory protection. In addition adsorption phenomena play a vital role in many solid-state reactions and biological mechanisms.

Adsorption is also used in the characterization of the surface properties and texture of fine powders. Many academic and industrial laboratories carry on

adsorption measurements on porous materials such as clays, ceramics, membranes and zeolites (Rouquerol et al, 1999). Adsorption is a powerful means of characterizing minerals, because the adsorption of a particular molecule gives information about the microporous volume, the mesoporous area and volume, the size of the pores, the energetic of adsorption and molecular transport (Malherbe, 2000).

2.1. Gas Adsorption

When a gas or vapor is brought into contact with a solid at a fixed pressure a decrease in the gas volume is observed, if the same procedure is applied at a fixed volume then a decrease in the gas pressure is observed. These observations show that the solid takes up part of the gas. The molecules that disappear from the gas either enter the inside of the solid, or remain on the outside attached to the surface. The former phenomenon is termed absorption and the latter adsorption. When both occur simultaneously, the process is termed sorption (Rouquerol et al, 1999).

Adsorption is related with the forces acting between the solid (atoms or ions composing the solid) and the gas molecules. All the gases tend to adsorb as a result of general van der Waals interactions with the solid surface giving rise to *physical adsorption (physisorption)* in which the interaction of the components of gas and solid pair is weak as in a condensation process. In the case of physisorption, there is concern about the degree of heterogeneity of the surface and with the extent to which adsorbed molecules possess translational and internal degrees of freedom. Sometimes the interaction of the components of gas and solid pair is strong as in a chemical reaction giving rise to *chemical adsorption (chemisorption)*. The adsorbate tends to be localized at particular sites (although some surface diffusion or mobility may still be present), and the equilibrium gas pressure may be so low that the adsorbent – adsorbate system can be studied under high – vacuum conditions (Adamson, 1990). The differences between chemisorption and physisorption may be expressed according to Rouquerol et al, (1999) as follows,

- Chemisorbed molecule may lose its identity on the solid surface as it undergoes a chemical reaction or dissociation and cannot be recovered by desorption, but physisorbed molecule keeps its identity and on desorption returns to the fluid phase in its original form

- As the temperature is increased, physisorption decreases while chemisorption increases.

- Chemisorption needs a special relation between the adsorptive – adsorbent pair, but physisorption may happen in any pairs at low temperatures due to its relatively low degree of specificity.

- Physisorption is quite fast and attain equilibrium rapidly, but chemisorption is related to the activation energy of the pairs and at low temperature the system may not have sufficient thermal energy to attain thermodynamic equilibrium.

- Chemisorption is necessarily to be limited to a monolayer, while physisorption may occur in one or multi layers (at high relative pressures).

Physisorption is more industrially preferred type of adsorption, because after the adsorption process, by desorbing the adsorbed gas, the adsorbent can easily be reused in another process. Gas that is chemisorbed may be difficult to remove, and desorption may be accompanied by chemical changes.

2.1.1. Adsorption Forces

The forces on adsorbate molecules are a function of distance between adsorbate and adsorbent atoms (pore size) and polarity (permanent or induced) of the adsorbate and adsorbent atoms. Physical forces that are responsible for the physical adsorption always include dispersion forces that are attractive, together with short-range repulsive forces. Also depending on the polar nature of the solid or the gas electrostatic (coulombic) forces also play role in the adsorption process. Dispersion forces, characterized by

London in 1930 considering the quantum mechanics, arise from the rapid fluctuation of electron density within each atom. This fluctuation in a gas molecule, which is approaching to the solid surface, induces an electrical moment and leads to attraction between the two atoms. Energy of interaction is expressed below,

$$\varepsilon_D (r) = -Cr^{-6} \quad (2.1)$$

C is the dipole – dipole dispersion constant

r is the distance between the two atom centers

Because of the interpenetrating of the electron clouds of the two atoms, short-range repulsive forces arise, and can also be derived from quantum mechanical considerations as,

$$\varepsilon_R (r) = B\, r^{-12} \quad (2.2)$$

B is the empirical constant

Therefore, the total potential energy between the two atoms becomes,

$$\varepsilon (r) = -Cr^{-6} + B\, r^{-12} \quad (2.3)$$

that is often called as Lennard- Jones potential.

In order to apply these equations to the adsorption of a gas on a solid surface, we need to consider the interaction of the solid surface, which is composed of atoms or ions with the molecules of the gas. Therefore the individual interactions of each solid atom with each gas molecule have to be added up to obtain the potential of a single molecule of the gas with reference to the solid.

$$\phi(z) = -C_{ij} \sum_j r_{ij}^{-6} + B_{ij} \sum_j r_{ij}^{-12} \quad (2.4)$$

In Eqn (2.4) r_{ij} is the distance between the molecule i in the gas phase (or, for a complex molecule, the center of its atom i) and the center of an atom j in the solid. In practice, only a limited number of atoms of the solid need to

be considered because of the rapid decreasing of potential with distance, implied by Eqn (2.3).

If the solid is polar in nature meaning that, if it consists of ions, or contains polar groups or π-electrons in it, then it will give rise to an electric field which will induce a dipole in the gas molecule. Then the interaction energy of ϕ_p will be added. If the gas molecule has a permanent dipole in addition, its interaction with the solid will result with a new energy as $\phi_{F\mu}$. Finally if the gas molecule possesses a quadrupole moment Q, this will produce a further contribution of ϕ_{FQ} to the energy. The interaction of the adsorbate-adsorbate pairs may also be included as the ϕ_{AA} term at the relatively high pressures, because of the forming of the multilayers on the solid surface.

Thus the overall interaction energy of a molecule at distance z from the surface may be expressed as adding up the interaction energies,

$$\phi(z) = \phi_D + \phi_R + \phi_p + \phi_{F\mu} + \phi_{FQ} + \phi_{AA} \qquad (2.5)$$

In Eqn (2.5) D and R represent the dispersion and repulsion forces respectively. These two contributions always exist, and where only these forces are involved it is called as nonspecific adsorption, while the other forces resulting from the electrostatic interactions may exist depending on the nature of the adsorbent and the adsorptive pair and therefore it is called specific adsorption where these contributions (some or all of ϕ_p, $\phi_{F\mu}$, and ϕ_{FQ}) are present in addition (Gregg and Sing, 1982).

2.1.2. Adsorption Isotherm:

The quantity of the gas taken up by the solid depends on the mass of the solid sample, temperature, pressure of the vapor, and the nature of the both the solid and the gas. Therefore if n represents the quantity of gas adsorbed in moles per gram of solid, then,

$$n = f(p, T, \text{gas}, \text{solid}) \qquad (2.6)$$

if the temperature is maintained constant, then eqn (2.6) simplifies to,

$$n = f(p)_{T,\ gas,\ solid} \qquad (2.7)$$

an alternative form may be used if the temperature is below the critical temperature of the gas,

$$n = f(p/p^{o})_{T,\ gas\ ,\ solid} \qquad (2.8)$$

here p^{o} is the saturation vapor pressure of the adsorptive.

Equations (2.7) and (2.8) are expressions of the *adsorption isotherm*. It gives the relationship between the amount of gas adsorbed and the pressure or relative pressure of the gas at a fixed temperature. Adsorption isotherms are very important in the subject of adsorption. After a detailed study of any isotherm, one can obtain all the necessary information about an adsorptive – adsorbent pair. Up to now thousands of adsorption isotherms were recorded in the literature. It was realized by Brunauer, Deming, Deming and Teller (BDDT) that most of those isotherms that result from physical adsorption may be grouped in to five classes (Fig 2.1) with Type VI, the stepped isotherm. A brief explanation about those groups is given below.

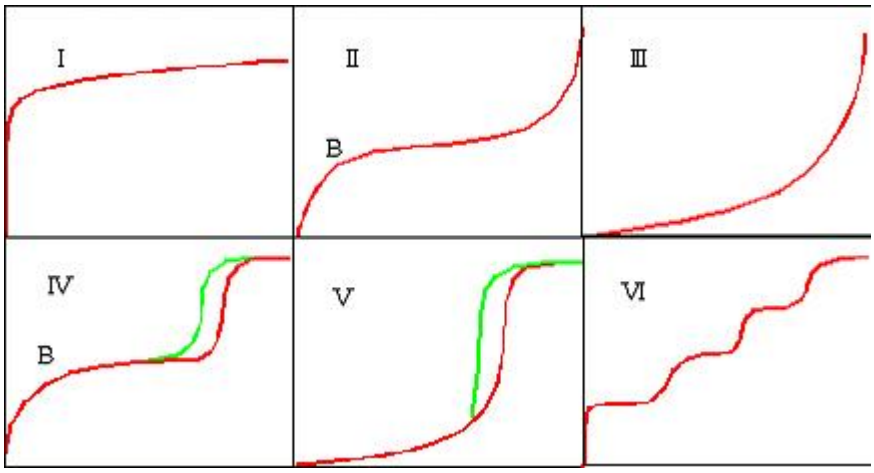

Figure 2.1. The six main types of gas physisorption isotherms

Type I is roughly characterized by a monotonic approach to a limiting adsorption that presumably corresponds to a complete monolayer and is observed by the physical adsorption of gases onto microporous solids and by the chemisorptions. Type II is very common in the case of physical adsorption and undoubtedly corresponds to multilayer formation. For many years it was the practice to take point *B*, at the knee of the curve, as the point

of completion of a monolayer, and surface areas obtained by this method are fairly consistent with those found using adsorbates that give type I isotherms. Type III is relatively rare, an example is that of the adsorption of nitrogen on ice, and seems to be characterized by a heat of adsorption equal or less than the heat of liquefaction of the adsorbate. Types IV and V are considered to reflect capillary condensation phenomena in that they level off before the saturation pressure is reached and may show hysteresis effects. Finally, the rare type VI steps-like isotherm is of particular theoretical interest and therefore has been included (Adamson, 1990, Gregg and Sing, 1982).

2.1.2.1. Langmuir Model

Several adsorption isotherms have been proven useful in understanding the process of adsorption. The simplest isotherm is attributed to a pioneer in the study of surface processes, Langmuir, and is called the Langmuir isotherm. It is based on the following assumptions,

1. Adsorption cannot proceed beyond the point at which the adsorbates are one layer thick on the surface (monolayer)

2. All adsorption sites are equivalent.

3. The adsorption and desorption rate is independent of the population of neighboring sites.

4. Heat of adsorption does not vary with the coverage

and the Langmuir equation is given:

$$p/n = 1/n_m b + p/n_m \qquad (2.9)$$

where n_m is the monolayer capacity, n (in moles) is the amount adsorbed on 11g of adsorbent and b is an empirical constant related to the condensation and evaporation rate constants. The Langmuir isotherm gives a simple picture of adsorption at low coverage; the amount adsorbed becomes proportional to the pressure and is applicable in some situations. At high

adsorbate pressures and thus high coverage, this simple isotherm fails to predict experimental results and thus cannot provide a correct explanation of adsorption in these conditions. Langmuir equation is more likely applicable to Type I isotherms for complete monolayer adsorptions on microporous solids and chemisorptions. A plot of p/n versus p should give a straight line, and the two constants n_m and b may be evaluated from the slope and intercept. The simple Langmuir model has retained great general utility as well as providing the point of departure for many of the proposed refinements.

Various attempts have been made to modify the Langmuir model. One of the best known is that of Fowler and Guggenheim in 1939, which allowed for adsorbate- adsorbate interactions in a localized monolayer on a uniform surface. However results turned out to be no more successful than the original Langmuir isotherm (Rouquerol et al, 1999).

2.1.2.2. BET Model

By adopting the Langmuir mechanism but introducing a number of simplifying assumptions, Brunauer, Emmett, and Teller in 1938 were able to arrive at their well known equation for multilayer adsorption, which has enjoyed widespread use ever since, and the result is named as the BET isotherm. The BET isotherm predicts that the amount of adsorption increases indefinitely as the pressure is increased since there is no limit to the amount of condensation of the adsorbate due to the main idea that the adsorbed molecules in one layer can act as adsorption sites for molecules in the next layer. Brunauer, Emmett, and Teller made three assumptions according to Gregg and Sing, (1982).

1. in all layers except the first the heat of adsorption is equal to the molar heat of condensation,

2. in all layers except the first the evaporation-condensation conditions are identical,

3. when $p = p^o$ (saturation vapor pressure), the adsorptive condenses to a bulk liquid on the surface of the solid, and the number of layers becomes infinite.

BET equation is given:

$$(p/p^o)/(n(1-p/p^o)) = 1/(n_m c) + (c-1)p/(n_m c p^o) \quad (2.10)$$

where c is a positive constant and is often assumed to be exponentially related to E_1 by the simplified equation:

$$c \approx \exp (E_1 - E_L) / RT \quad (2.11)$$

Here, E_1 is defined as a positive quantity and interpreted as the ' average heat of adsorption on the *less active* part of the adsorbing surface', which is the first layer according to the BET model. $E_1 - E_L$ was originally known as the ' net heat of adsorption' but it is recommended that the more general term 'net molar energy of adsorption' should be adopted (Rouquerol et al, 1999).

If plotted as n/n_m against p/p^o, Eq (2.10) gives a curve having the shape of a Type II isotherm, which also has been called an S-shaped or sigmoid isotherm. However if C<2, the shape is changed and the point of inflection is lost. The BET equation then gives a Type III isotherm. Therefore the shape of the knee depends on the c value and becomes sharper as the value of c becomes greater. Thus for c large, that is $E_1 >> E_L$, it reduces to the Langmuir equation (Adamson, 1990). An interesting feature of the BET equation is that it allows for the possibility that when the surface is covered with a 'statistical monolayer', a fraction still apparently remains uncovered and this fraction $(\theta_o)\ n_m$ is directly dependent on the value of c:

$$(\theta_o)\ n_m = 1/(\sqrt{c} + 1) \quad (2.12)$$

which means that the higher the c value, the smaller the uncovered fraction of the surface when the statistical monolayer is achieved. For c values of 1, 9 and 100, the corresponding fractions of uncovered surface are given as 50 %, 25 % and 10 % by Rouquerol et al, (1999). Therefore for the systems with low c values, the BET monolayer capacity cannot be relied on to give a realistic assessment of the magnitude of the total area of the surface. Furthermore, the quantity c must be positive; any negative intercept on the ordinate of the BET plot is an indication that we are outside the valid range of the BET equation.

The Langmuir isotherm is found to be useful only at very small coverages (sub-monolayer) but is generally applied to all cases involving chemisorption. This would correspond to the limiting case of c approaching infinity in the BET formalism. The BET isotherm is found to describe adequately the physisorption at intermediate coverage but fails to represent observations at low or high coverage. Linear region of a plot according to Eq 2.10 typically lies between a p/p^o of 0.05 and 0.3. The typical deviation is such that the best-fitting BET equation predicts too little adsorption at low pressures and too much at high pressures.

In spite of the unrealistic appearance of the theory due to the assumptions made, the BET equation remains the most used of all adsorption isotherm equations. A recent molecular simulation study by Seri-Levy and Avnir in 1993 has also revealed the artificial nature of the BET model and has illustrated the effect of taking adsorbate-adsorbate interactions into account. Thus, the addition of lateral interactions appears to flatten the BET stacks into more realistically shaped islands (Rouquerol et al, 1999).

2.1.2.3. Dubinin Model

Dubinin was the pioneer of the concept of micropore filling. According to Dubinin's ideas, the process involved is volume filling of the micropores rather than layer-by-layer adsorption on the pore walls. His approach was based on the potential theory of Polanyi, in which the physisorption isotherm

data were expressed in the form of a temperature-invariant characteristic curve. This different approach to multilayer adsorption considered that there is a potential field at the surface of a solid into which adsorbate molecules fall. Dubinin and Radushkevich put forward an equation for the characteristic curve in order to estimate the micropore volume from the low and medium pressure parts of the adsorption isotherm in terms of the fractional filling, W/W_o, of the micropore volume, W_o. This relation is usually expressed in the form

$$W/W_o = \exp [- (A/E)^2] \qquad (2.13)$$

where A, 'the Polanyi adsorption potential', is an adsorption affinity,

$$A= -RT \ln (p/p^o) \qquad (2.14)$$

E is a characteristic free energy of adsorption for the given system, W is the amount adsorbed expressed as a liquid volume and is given by $W= n/p^*$ where p^* is the density of the adsorbate in the micropores.

In an attempt to extend the scope of the DR treatment, Dubinin and Astakhov have put forward a more general equation, which is based on a Weibull rather than a Gaussian distribution of pore sizes (Gregg and Sing, 1982):

$$W/W_o= \exp [- (A/E)^n] \qquad (2.15)$$

where n is an empirical constant. Thus the original DR equation is a special case of the Dubinin – Astakhov equation, with n = 2. Dubinin reported values of n between 2 and 6. Some molecular sieve carbons and zeolites gave n=3. The particular value of n may also depend on the range of the isotherm and the operational temperature.

For determining the pore size distribution of a microporous adsorbent, currently there is no standard (Gregg and Sing, 1982). Several models have been proposed and all of them rely on using adsorption isotherm data of a single adsorbate and then converting that adsorption data into a pore size distribution. Because of the assumptions made in their derivations. it is very

likely that none of the methods give a true representation of the pore size distribution of a microporous adsorbent. One of the method used in finding the pore size distributions is Horwath-Kawazoe (HK) method. This method was developed in 1983 for determining effective pore size distributions from adsorption isotherms on molecular-sieve activated carbon. HK model was initially for slit-shaped pores using N_2 isotherms at 77 K, but it can be extended to other pore shapes and other adsorbates, using slight modifications to the model, given by the equation:

$$\ln(p/p^o) = \frac{61.63}{(H-0.64)}\left[\frac{1.895\times10^{-3}}{(H-0.32)^3} - \frac{2.709\times10^{-7}}{(H-0.32)^9} - 0.05014\right] \qquad (2.16)$$

where H (width of uniform slits within a graphitic structure) is expressed in nm.

2.2. Adsorbents

There are many kinds of adsorbents used in industry based on gas adsorption processes for many years such as activated carbon, silica gel, membranes, activated alumina, natural and synthetic zeolites, etc. The older types of adsorbents such as activated carbons and silica gels are generally non crystalline and their surface and pore structures tend to be ill-defined and difficult to characterize. However there is a growing number of adsorbents having intracrystalline pore structures such as zeolites and aluminophosphates. Also great developments are being shown in the design of other new materials having pores of well-defined size and shape. Special interest will be given on natural zeolites in this study since they exist in huge amounts in Turkey and deserve special attention because of their characteristics.

2.2.1. Natural Zeolites

Natural zeolites were discovered by Freiherr Axel Fredrick Cronsted, a Swedish mineralogist, during the collection of minerals in a copper mine in Lappmark, Sweden. Cronsted named the new material as zeolite because of the characteristics of the mineral observed by him during blowpipe tests.

The name is derived from two Greek roots “zeo” to boil and “lithos” a stone describing the zeolite behavior under fast heating conditions, when the zeolite minerals seem to boil because of the fast water loss. Since Cronsted’s initial discovery of stilbite, more than 50 natural zeolites have been detected. In fact, mankind knew these unique minerals for centuries before the Cronsted’s recognition of them as a distinct mineralogical species. They were used as dimension stones in the construction of pyramids and temples in Mexico and of houses and churches in Cappadoccia and were also used by Romans for the production of pozzolanic cement. (Malherbe, 2001). The use of natural zeolites for other purposes was started in Japan and the United States during the 1950s and afterwards in other countries (Malherbe, 2001).

Natural zeolites are mostly found in regions of former or present magmatic activity, which means that high temperature, and the presence of water influenced the formation. During the cooling process of a magmatic intrusion, the dissolved reminding ions, water vapor, carbondioxide and other volatile compounds are separated trying to reach the earth surface. This volatile phase also called fluid phase crystallizes during the cooling process loosing its high pressure. Different stages of crystallization can be observed during the loss of temperature and pressure. Only at the lowest stage of pressure and temperature, at the mildest conditions called the hydrothermal state, the formation conditions for aluminosilicate zeolite phases are reached. In nature this can be achieved not only by crystallization of the volatile phase itself in cavities, but also by intrusion into neighboring aluminosilicate beds transforming the material partially to zeolites. Even at the lowest pressures like in hot springs the formation of zeolites can be observed (Ghobarkar et al, 1999).

Zeolites were defined as aluminasilicates with a skeletal structure, containing voids occupied by ions and molecules of water having considerable freedom of movement (Tsitsishvili et al, 1992). The aluminosilicate framework is the most conserved and stable component of the zeolites and defines the structure type. The topology of the framework,

the numbers and distribution of charges are basically formed at the crystal growth stage. (Tsitsishvili et al, 1992). The extraordinary properties of zeolites are caused by their crystal lattice. A proper classification starts from the 3-dimensional bonding of the tetrahedrally coordinated framework cations. Today about 800 different zeolites are known which can be classified by 119 different zeolite structure types. Only about ¼ of them are naturally occurring, the others are synthetic (Ghobarkar et al, 1999).

The primary building block of the zeolite framework is the tetrahedron (Figure 2.2), the centre of which is occupied by a silicon or aluminium atom, with four atoms of oxygen at the vertices. Each oxygen atom is shared between two tetrahedra. Hence, the tetrahedra form a continuous framework. The negative charge of the framework is defined by the substitution of Si^{4+} by Al^{3+}, which is compensated by mono and/or divalent cations together with water molecules in structural channels (Tsitsishvili et al, 1992).

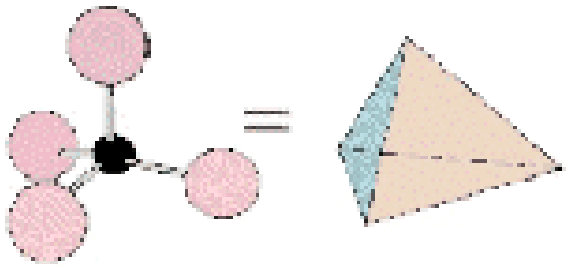

Figure 2.2. An $[SiO_4]$ or $[AlO_4]^{1-}$ tetrahedra (primary building unit)

The general chemical formula unit of zeolites is given below:

$$Me^{z+}_{(m/z)}\,[Al_m \,.\, Si_n \,.\, O_{2(n+m)}\,] \,.\, qH_2O \qquad (2.14)$$

With Me as the extraframework cations (e.g. Li^+, Na^+, K^+,…..,Ca^{2+}, Sr^{2+},…), z the charge of cations, framework ions in brackets, m as the number of Al per formula unit, n the number of Si per formula unit and q the number of water molecules in the cavity system (Ghobarkar et al, 1999). The Si/Al ratio in natural zeolites lies within the limits of 1 to 6. The lower limit is determined by Loewenstein's rule according to which an AlO_4 tetrahedron cannot associate with another AlO_4 tetrahedron by a common

oxygen atom; at Si/Al = 1, the silicon and aluminum tetrahedra alternate to form the ordered framework (Tsitsishvili et al, 1992).

Four different positions of extraframework cations of zeolites are possible. At the first position the cation is only coordinated by framework oxygens. At the second, the cation is coordinated by framework oxygens at two nearly opposite sides together with some water molecules. At a third possible position, the cation is bound one sided to framework oxygen and on the other side by water molecules. A fourth possible position is the completely surrounding of the cation by water molecules (Ghobarkar et al, 1999).

The crystalline framework contains cages and channels. Under ordinary conditions, the channels are filled with cations and water molecules. Cation-oxygen atom and cation-water molecule distances cover rather wide ranges as compared with the tetrahedral interactions and depend mainly upon the size of the cation. Cations are bound more strongly by water oxygen than by framework oxygen atoms. (Tsitsishvili et al, 1992). Zeolite channels are classified according to the number of oxygen or tetrahedral or framework (T) atoms forming the window together with the geometrical dimensions of the two-dimensional channel opening. Per definition the minimum T atoms necessary to build up a channel is six but even a four membered ring is actually a gateway to a channel. Up to 20 membered rings exist as channel openings (Ghobarkar et al, 1999). The cross-section of the opening may be ring-shaped, elliptical, drop-shaped or asymmetrically shaped. Channel systems can be one-, two- or three- dimensional. Different kinds of arrangements of 3-dimensional channel systems exist, such as tetrahedral, octahedral, hexahedral, trigonal and hexagonal. The sizes of the channel openings are dependent on water content and/or cation species present in the channel system and with dehydration the dimensions of the channels change making the zeolite structures flexible. Zeolite cages are as important for the zeolite specific properties as the channel systems are. The channels themselves are also cages of infinite length. Cages can be defined as voids bigger in diameter than normal channel systems. They are only accessible

through the channel system. The simplest cages are formed at the crossing of two channel systems. (Ghobarkar et al, 1999).

The water content of the zeolites varies within certain limits depending upon the character of the exchange cations and conditions of crystallization. Under ordinary conditions the water molecules completely fill the free volume of channels and voids in the zeolite structure. The free inner volume of the zeolite can be calculated by measuring the volume of water released under heating in *vacuo*. Experience shows that the volumes calculated by this method agree well with structural data (Tsitsishvili et al, 1992). The number of water molecules present is defined only by the space accessible; substitution of two Na^{+} ions by one Ca^{2+} ion allows the introduction of one more water molecule. Between polar water molecules and the framework system, dipole forces act the one hand side. On the other hand side water molecules on well defined crystallographic places act as solvent for the present extraframework cations dependent on charge distribution of the zeolite framework caused by (Si, Al) distribution together with the charge distribution within the void system. This binding state of water in zeolites is typical for this class of solid-state minerals, therefore the term 'zeolitic' water is used (Ghobarkar et al, 1999).

In mineralogical terms water is called "zeolitic" when it can be removed at elevated temperature without destruction of the original structure and which can absorb once more on recovery of original conditions (Tsitsishvili et al, 1992). Zeolite water is represented in the crystals by H_2O molecules, but the properties and the state of this component differ essentially in various structures. According to Tsitsishvili et al, (1992), the roles of the water molecules in zeolites can be counted as:

- to complete the coordination of the cations in the cavities
- to minimize electrostatic repulsion between the framework oxygen atoms
- to act as stabilizer the porous structure of the aluminasilicate structure

2.2.1.1. Purification and Modification of Natural Zeolites

Around thirty years ago the natural zeolites were called " the mineral of the century" (Malherbe, 2001). But at present, after the synthetic zeolite industry has developed, competition between natural and synthetic zeolites became harder. Natural zeolites occur in huge masses and are cheaper than the sol-gel derived synthetic ones but there is always the problem of impurities. As well as the water soluble Ca, or Na compounds, Fe and also sometimes toxic ions like Ba are present in the channel system. In order to be more effective, natural zeolites should be cleaned and modified by physical and chemical means prior to use. Natural zeolites can be cleaned to high purity using currently available mineral processing equipment, such as jaw crushers, crushing rolls, hydrocylones, classifiers, and shaking tables. Using these techniques and utilizing the differences in hardness, density, and particle size between the zeolite phase in the rock it is possible to concentrate the zeolite phase in the final product (Malherbe, 2001). Heating in distilled water is applied to natural zeolites to remove the water-soluble impurities. Besides washing, dispersion in methyl iodide (Ackley and Yang, 1991), and bromoform + carbon tetrachloride mixture (Esenli, 1993) are also applied to remove the heavy impurities. The simplest manipulation necessary for the use of a zeolite as an adsorbent is its dehydration. Water molecules in zeolites are held with a pseudo-continuous range of energies: some water molecules are desorbed at relatively low temperatures, and the rest are firmly held to the extraframework cations and often evolve with concomitant cationic migration and structural relaxation (Malherbe, 2001). Some zeolites such as clinoptilolite and mordenite can be heated up to 300-400 ^{o}C and completely dehydrated without loss of crystallinity, but other zeolites, such as scolecite and natrolite undergo transformations during dehydration. Natural zeolites, after the elimination of zeolitic water by heating, are capable, on account of their structure, of adsorbing gases and vapors in the zeolite primary porosity that is in the cavities and channels that constitute the zeolite framework. Moreover, adsorption also takes place

in the zeolite secondary porosity, which includes the macro and mesoporosity of zeolite rocks, shaped by the matrix between the zeolite crystals.

Behaviour of the natural zeolites can be modified by the number, location and size of the intracrystalline cations which neutralize the negative charge on the framework. It is well-known fact that the cationic composition of the zeolites directly affects the adsorption capacity in the primary porosity of these materials. This makes it possible to regulate the properties of natural zeolites by ionic exchange. These exchange processes are done mostly by the cations named as Ca^{2+}, Na^{+}, K^{+}, Li^{+}, Cs^{+}, Rb^{+}, Mg^{2+} (Malherbe, 2001, Ghobarkar et al, 1999, Armbruster, 2001). Changing the cations in a zeolite may effectively enlarge the pore openings by diminishing the cation population (Vansant and Cool, 2001). Pore size engineering in zeolites can also be achieved by modification of the zeolite framework resulting from the internal and external structural modification by implantation of additional atom groups and external surface modification of the zeolite crystal by coating (Vansant and Cool, 2001).

Deamination is another modification way applied in zeolites previously exchanged with ammonium cations; they are transformed into acid zeolites by the decomposition of the exchanged ammonium cations. This procedure may be followed by ultrastabilization, which is one of the basic operations in the industrial production of acid catalysts, consisting in controlled dealumination produced by thermal treatment in water-vapor atmosphere, which increases the thermal stability of the zeolite (Malherbe, 2001).

Another method is the thermal reduction in which the zeolite is exchanged with the cationic form of the metal and afterward the obtained exchanged zeolite is reduced in H_2 atmosphere at 450 ^{o}C and maintained at that temperature for about 2h (Malherbe, 2001).

Thermal treatment is one of the major methods for dislodging aluminium from framework to non-framework positions in zeolites. In the thermal or hydrothermal treatment of zeolites, the non-framework aluminium species

stay in the zeolite channels, while the framework Si/Al ratios increase (Hong and Fripiat, 1995).

Another and mainly used procedure for altering the adsorption properties of natural zeolites is leaching them with mineral acids The acid treatment exchanges cations of the zeolite with H^+ and causes dealumination of the zeolite structure (Malherbe, 2001). The presence of large amounts of extraframework aluminium has a detrimental effect on catalytic and transport properties so that it is usual to extract the aluminium by a subsequent chemical attack. Mineral acid attack to remove extraframework aluminium is common industrial process (Gola et al, 2000). Acid treatment has often been used to modify either natural or synthetic zeolites for several purposes, among which the replacement of the native cations by H^+ ions and the dealumination of the zeolite framework are the main ones (Notario et al, 1995). Dealumination may cause the partial or complete destruction of the zeolite framework as well. Acid treatment also causes some modifications in the zeolite morphology, by destructing the channel blocking impurities and developing the secondary porosity (Malherbe, 2001).

In the acid leaching process of zeolites, the cations are easily replaced with H_3O^+ ions by mild acid treatment. This exchange establishes the equilibrium,

$$[\equiv Si\text{-}O\text{-}Al^- \equiv]\ H_3O^+ \quad [\equiv Si - O^{\delta+} - H \qquad Al^{\delta-} \equiv] + H_2O \quad [\equiv Si - OH$$

At low SiO_2 / Al_2O_3 ratio, the concentration of broken SiO-Al bonds is so high that the structure collapses, as the bridging oxygen competes with the water for the proton. The water molecule is then chemisorbed on the Al Lewis acid site, thereby beginning the hydrolysis process. Reaction can be enhanced by heating and leads to the conversion of framework-Al to cationic hydroxylated aluminum. However, the hydroxylated aluminium cations formed in the hydrolysis reaction protect remaining framework-Al from hydrolytic attack. The hydoxylated aluminum cation can react further with acid sites neutralizing the hydroxyl groups of the cationic Al species to

yield $Al(OH)^{2+}$ and Al^{3+} ions which are exchanged for H_3O^+ and the dealumination proceeds (Weitkamp and Puppe, 1999). The first acid extraction of a zeolite was reported by Barrer and Makki who treated clinoptilolite with HCl and found that, in addition to the cations, framework aluminum was progressively removed. Without loss of crystal structure, a product without a framework charge was eventually obtained (Weitkamp and Puppe, 1999).

The type of the acid, the acidity of the solution, the duration and temperature of leaching, crystal size, original crystal structure and composition have all strong influences on leaching and any variations in these parameters may be effective to the zeolite structure. As the Si/Al ratio increases, the cation density decreases. Therefore the adsorption capacity of zeolites for various gases changes. Acid leaching of a natural clinoptilolite increases the adsorption of nonpolar molecules such as benzene but decreases the adsorption of polar molecules such as water (Malherbe, 2001).

The most used strong acids for the dealumination of zeolites can be named as HCl, HNO_3, and H_2SO_4. Leaching of zeolites with weak acids such as H_3PO_4 opens possibilities for the removal of impurities such as carbonates or iron and for the improvement of the cationic composition of the sample with low dealumination and with a smaller decrease of crystallinity than with strong acids like HCl (Malherbe, 2001). Notario et al (1995) characterized the H_3PO_4 (1 N, 2 N and 3 N) treated phillipsite from southern Tenerife with 24 h shaking time at room temperature and detected significant loss of crystallinity which is probably a good example pointing out the importance of the duration of leaching. Pozas et al, (1996) noted that the clinoptilolite from the deposits of Castillas treated with H_3PO_4 (4 M) for 5-40 min at 100 ^oC, retained its crystallinity after the treatment. Partial and strong dealuminations of the framework and loss of zeolite phase of natural clinoptilolites treated with HCl were also reported before (Iznaga et al, 2002). By using 2 M HCl, decreasing Al concentration in the clinoptilolite framework, and by using 1 and 2 M HCl, decreasing Al concentrations and

partial surface amorphization in the natural heulandite framework were observed after 48 h treatment. Subsequent X-ray single-crystal structure analysis indicated that partial rearrangement of framework Al to hydrated extraframework Al occured, where Al preferred octahedral coordination. Thus not only H_3O^+ but also Al^{3+} appeared as extraframework cations (Armbruster, 2001). Usage of HNO_3 and H_2SO_4 in order to enhance the adsorption capacities of the zeolites was also mentioned by Notario et al (1995).

2.2.2. Clinoptilolite

Since its introduction into the literature in 1923, clinoptilolite has been a subject of confusion within the zeolite group of minerals (Mumpton, 1960). Heulandite was one of the first zeolites described and has been investigated for more than two centuries. The history of investigation of clinoptilolite is shorter, but eventful. The first example of clinoptilolite was mentioned by Pirson in 1890, but it was incorrectly described as mordenite on the basis of chemical analysis. Schaller described clinoptilolite as a separate mineral species in 1932. Hay and Bannister led to the conclusion that clinoptilolite could be regarded as 'high-silica' heulandite. Clinoptilolite as a mineral species was redefined by Mumpton in 1960 on the basis of the chemical, optical, X-ray and thermal properties of a sample from volcanic tuff (Tsitsishvili et al, 1992).

Clinoptilolite is the most abundant of the natural zeolites. Compositions and purity vary widely among the many deposits found throughout the world (Ackley and Yang, 1991). Such deposits are commercially important because clinoptilolite tuffs are often rather pure and can be mined with simple techniques. Approximately 25 years ago 300000 tons of zeolitic tuff were mined per year. In 1997 3.6 million tons of natural zeolites (mainly clinoptilolite and chabazite) were worldwide produced (Armbruster, 2001).

Western Anatolia, in Turkey, has very large clinoptilolite reserves and Gördes and Bigadiç are the most known regions as clinoptilolite reserves (Yaşyerli et al, 2002). Bigadiç region has one of the most clinoptilolite

occurrence in Turkey with an estimated reserve of 2 billion tons (Abusafa and Yücel, 2002).

Clinoptilolite is defined as the zeolite mineral series having the distinctive framework topology of heulandite (HEU) and it differs from heulandite in having higher Si/Al ratio. Clinoptilolite has a Si/Al ratio > 4 while heulandite has a ratio Si/Al < 4 (Malherbe, 2001). The key difference between heulandite and clinoptilolite is thermal stability. Clinoptilolite is thermally stable to temperatures in excess of 500 °C, while heulandite undergoes structural collapse at 350 °C (Malherbe, 2001). Transformation of heulandite into another phase around 250- 350 °C was also noted by Mumpton, (1960), and Tsitsishvili et al, (1992). According to Mumpton, (1960) high temperature X-ray diffraction studies clearly identifies the two minerals.

The structural topology of the tetrahedral HEU framework is well understood and possesses C 2/m space group symmetry with oblate channels confined by ten-membered (7.5 × 3.1 Å) and eight-membered tetrahedral rings (4.6 × 3.6 Å) parallel to the c-axis. Additional eight-membered ring channels (4.7 × 2.8 Å) parallel to [100] and [102] cross-link the former channels within (010), forming a two-dimensional channel system. The unit cell is monoclinic and is usually characterized on the basis of 72 O atoms and 24 water molecules, with Na^+, K^+, Ca^{2+}, and Mg^{2+} as the most common charge-balancing cations. Representative unit cell parameters for the $(Na, K)_6$ $(Al_6Si_{30}O_{72}).20H_2O$ form are a=1.762 nm , b=1.791nm, c=0.739nm, β=2.029 rad (Ackley and Yang, 1991).

The clinoptilolite crystalline structure have a series of intersecting channels, each layer of channels separated by a dense gas-impermeable layer of tetrahedral framework forming a 2-Dimensional microporous channel system with elliptical pore openings. Channel A (10-membered ring) and B (8-membered ring) are parallel to each other and the c axis of the unit cell, while the C channel (8-membered ring) lies along a axis, intersecting both the A and B channels (Figure 2.3). The selectivity and rate of uptake of

gases are strongly influenced by the type, number, and location of the charge-balancing cations residing in the A, B, and C channels. Cation sites, as determined for clinoptilolite and the estimated dimensions of the elliptic channels are summarized in Table 2.1 (Ackley and Yang, 1991).

Table 2.1. Channel Characteristics and Cation Sites in Clinoptilolite

Channel	tetrahedral ring size/channel axis	cation site	major cations	Approximate channel dimensions,nm×nm
A	10/c	M(1)	Na, Ca	0.72×0.44
B	8/c	M(2)	Ca, Na	0.47×0.41
C	8/a	M(3)	K	0.55×0.40
A	10/c	M(4)	Mg	0.72×0.44

Small hydrated cations (Na^+, K^+, Ca^{2+}, and Mg^{2+}) can easily enter the channels of clinoptilolite and compete for the major exchangeable cation sites, designated as M(1), M(2), M(3), and M(4) (Armenta et al, 2001). Na^+ is surrounded by 5 water molecules and 2 framework oxygen atoms in M(1), and surrounded by 5 water molecules and 3 oxygen atoms in M(2). At the same time, K^+ occupies the M(3) positions, with 6 oxygen atoms and 3 water molecules as nearest neighbours Mg occupies the M(4) positions, with the surroundings of 6 water molecules (Tsitsishvili et al, 1992). The amount of magnesium in clinoptilolite approaches in some cases one cation per unit cell. Sodium, calcium and potassium ions have a mixed coordination sphere of water molecules and framework oxygen atoms, whereas magnesium is octahedrally coordinated by water molecules (Tsitsishvili et al, 1992).

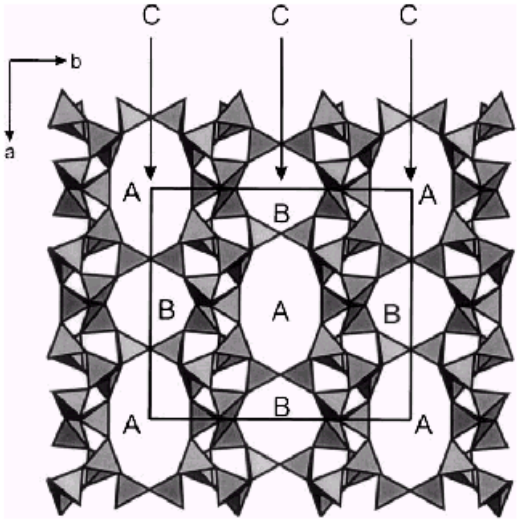

Figure 2.3. Tetrahedral model of the heulandite framework projected along the c – axis, showing the ten-membered A and the eight-membered B channels. Eight-membered C channels, indicated by arrows connect A and B channels.

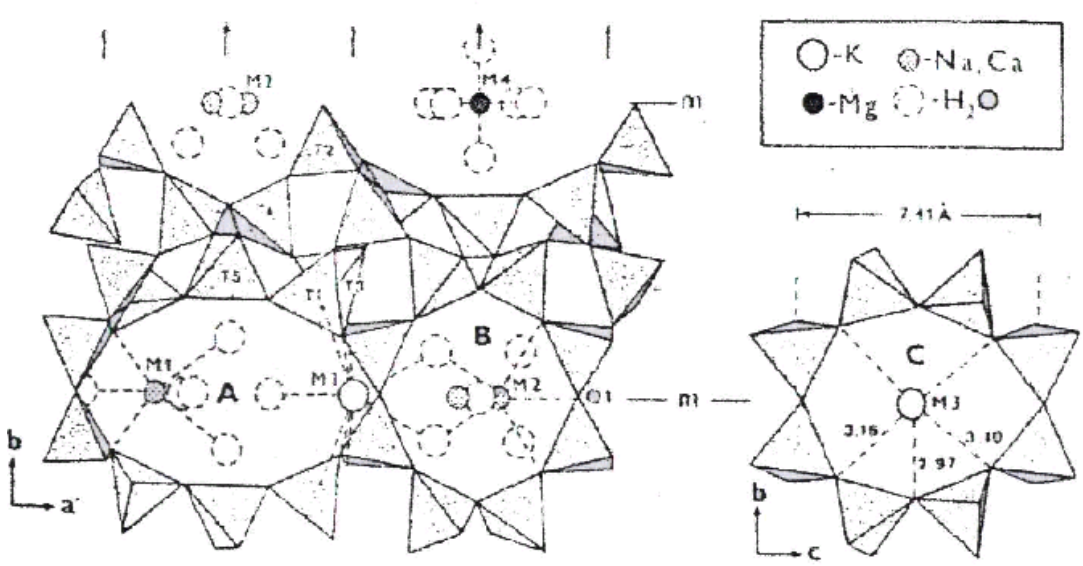

Figure 2.4. The c-axis projection of the structure of clinoptilolite, showing the cation positions in the structure.

The major cations are located and distributed in Fig 2.3 are as follows: M(1) is located in channel A where Na>Ca; M(2) is located in channel B where Ca>Na.

M(3) is located in channel C, where there is only K; and M(4) is located in channel A, where there is only Mg (Armenta et al, 2001).

During the adsorption process in zeolites, initial micropore filling (adsorption in the primary porosity) is followed by surface coverage on the walls of open mesopores and macropores (adsorption in the secondary porosity), which occurs at higher pressures and comprises monolayer, multilayer adsorption and capillary condensation (Malherbe, 2001).

When a molecule diffuses inside a zeolite channel, it is attracted and repelled by various interactions, such as the dispersion energy (ϕ_D), repulsion energy (ϕ_R), polarization energy (ϕ_P), field dipole energy ($\phi_{E\mu}$), field-gradient-quadrupole interaction (ϕ_{EQ}), and sorbate – sorbate interactions (ϕ_{AA}) as discussed in detail before. For the molecules with high dipole moments such as H_2O, H_2S, SO_2, and NH_3 and for the molecules with high quadrupole moment such as CO_2, the electrostatic interactions are stronger than the dispersion plus repulsion interactions. But for the molecules such as Ar and CH_4 the main forces present during the adsorption are the dispersion and repulsion forces. In the adsorption of N_2 and O_2, the dipole moments of these molecules are zero and the quadrupole moments are very low (Malherbe, 2001).

2.3. Application Areas of Zeolites

Zeolites have basically become interesting because of their applicability in almost all fields of human life where chemical, biochemical, and physicochemical processes are taking place. The utilization of the properties of natural zeolites in industry, agriculture, environmental protection, and animal nourishment and health transformed natural zeolites from the late 1960s into the mineral of the century, and various mining companies went into the natural zeolite business. After the reports of agricultural, environmental and industrial applications in Japan during the early and mid 1970s, natural zeolites were considered as wonder materials. Commercially feasible deposits of zeolites in the world have been discovered in Australia, Bulgaria, Canada, Cuba, Georgia, Hungary, Italy, Japan, Mexico, Romania, Russia, Serbia, Slovakia, Turkey, Ukraine and the United States. Occurrences have been reported in Angola, Argentina, Botswana, Burundi, Chile, Egypt, Germany, Guatemala, France, Iran, Kenya, Korea, Nicaragua,

Pakistan, Panama, the Philippines, Spain, the South African Republic, and Tanzania (Malherbe, 2001).

In the last 40 years, zeolites both natural and synthetic have become the most important materials in modern technology. Today, the production and application of zeolites for industrial processes is a multimillion-dollar industry (Malherbe, 2001). Zeolites can be used for purification of gaseous as well as liquid mixtures and solutions by sorption, sieving and filtering, for storing of molecules, for ion exchange purposes and catalysis under nonoxidizing and oxidizing environments (Ribeiro et al, 1984).

2.3.1. Adsorption Applications of Zeolites

The study of zeolites as adsorbent materials was initiated by Prof. Richard M. Barrer in 1938, when he published the paper " Sorption of Polar and Non-polar Gases by Zeolites " and started the publication of a series of papers on the adsorptive properties of zeolites, where he confirmed the molecular sieving character of zeolites. Prof Barrer not only initiated the study of zeolites as adsorbents but also understood the usefulness of these minerals in many applications, and can be considered as the father of the zeolite science and technology (Malherbe, 2001).

Natural zeolites are good adsorbents for H_2O, NH_3, H_2S, NO, NO_2, SO_2, CH_3OH, CO, and CO_2 (Malherbe, 2001). The specific interactions between the zeolite framework and the molecules having high dipole or quadrupole moments (H_2O, H_2S, SO_2, CO_2, NH_3) are responsible for the use of zeolite for gas drying, NH_3 removal (Helminen et al, 2000), and purification of air or other gases by the removal of pollutants such as CO_2, SO_2, and H_2S (Rege et al, 2000, Malherbe, 2001, Ghobarkar et al, 1999, Armbruster, 2001). Also, the differences in the quadrupole moments between N_2, CH_4, and O_2 are the basis for the use of zeolite adsorption for the separation of N_2 and O_2 (Talu et al, 1996) and N_2 and CH_4 (Ackley and Yang, 1991, Huesca et al, 1999) in mixtures. The separation of air into N_2 and O_2 is very important for N_2 is the second largest volume chemical produced by industry and O_2 the fourth. Based on the selective properties of some natural zeolites such as chabazite,

clinoptilolite, and mordenite for nitrogen, these zeolites can be used for the N_2-O_2 separation with a better performance than the synthetic mordenite or type A zeolites (Malherbe, 2001). The solar energy storage and solar cooling applications of natural zeolites are closely connected with the adsorption properties of these minerals. According to Ribeiro et al, (1984) commercial adsorbent applications of zeolites may be summarized in two groups:

A. Purification:

1. Drying: natural gas, cracked gas, insulated windows, refrigerant
2. CO_2 removal: natural gas, cryogenic air separation
3. Sulfur Compound Removal: sweetening of natural gas and LPG
4. Pollution Abatement: removal of Hg, NO_X, SO_X.

B. Bulk Separations**:**

1. Normal/ iso-paraffin separation
2. Xylene separation
3. O_2 from air

Purification applications generally depend on surface selectivity for polar or polarisable molecules such as water, CO_2 or surface compounds, and bulk separations are generally based on molecular sieving principles.

2.3.2. Catalysis Applications of Zeolites

Fundamental discoveries in the use of zeolites in hydrocarbon catalysis were made in the 1950's. Developments in zeolite catalytic cracking have occurred both in materials and process. Some industrial processes that utilize zeolite-based catalysts are alkylation, cracking, hydrocracking, isomerization, hydrogenation and dehydrogenation, hydrodealkylation, methanation, and some inorganic reactions. All are based on the unique properties of zeolite catalysts, which have in common, extremely high strength acid sites, and selectivities related to strong adsorptive forces within the zeolite (Ribeiro et al, 1984).

2.3.3. Ionic Exchange Applications of Zeolites

Another unique property of the zeolites is the selective cation exchange. The applications of ionic exchange in natural zeolites, after the rediscovery of these minerals in the late 1950s, started with the studies carried out by Ames and coworkers, who discovered that chabazite, clinoptilolite, and mordenite are excellent exchangers for Cs^{+}, Sr^{2+}, Rb^{+}, K^{+}, and NH_4^{+} (Malherbe, 2001). Cation exchange of zeolites is used routinely in modifying the properties of zeolite products used in adsorption and catalysis. Ion exchange applications of zeolites can be counted as,

- Removal of Cs^{+}, and Sr^{2+} radioisotopes by mordenite and clinoptilolite
- Removal of NH_4^{+} from wastewater by clinoptilolite
- Radioactive waste storage
- Aquaculture
- Regeneration of artificial kidney dialysate solution
- Metals removal and recovery
- Ion exchange fertilizers
- Detergent builder

Natural zeolites have played an important role in the development of ion exchange applications. The use of zeolite minerals chabazite, mordenite and clinoptilolite for the removal of cesium and strontium radioisotopes in the nuclear industry was among the earliest applications of zeolites as ion exchangers. Their superior selectivity and stability characteristics spurred the development of other zeolite ion exchange applications (Ribeiro et al, 1984). During the Chernobyl disaster thirty to forty times the radioactivity of the atomic bombs dropped on Hiroshima and Nagasaki were released. The main radioactive isotopes from the Chernobyl accident were ^{137}Cs, ^{134}Cs, ^{90}Sr, and ^{89}Sr. The details of zeolite applications at Chernobyl remain rather obscure because of a secrecy problem still remaining after disintegration of the former Soviet Union. About 500,000 tons of zeolite rocks, mainly containing clinoptilolite, were processed at various deposits in Ukraine, Georgia, and Russia specifically for use at Chernobyl. The

majority of the zeolites were used for the construction of protective barriers and for agricultural applications in polluted areas (Armbruster, 2001). In addition, filters of clinoptilolite tuffs were suggested to extract radionucleides from the drainage water of the encapsulated Chernobyl nuclear power plant. Filtration reduced Cs by 95 % and Sr by 50-60 %. To reduce Cs radionucleides in cow milk in Bulgaria, 10 % clinoptilolite was added to the cow feed resulting in 30 % Cs reduction in the milk. In Western Europe clinoptilolite was tested to reduce radionucleide levels in soil, plants, sheep and fruit juice. Pilot studies of NH_4^+ removal from municipal wastewater by using clinoptilolite-containing tuff were reported from various countries. After exchange and subsequent regeneration of the zeolite with NaCl / KCl solutions, ammonia was stripped from the solution and an ammonium-phosphate fertilizer was produced. Ca-saturated clinoptilolite was used for ammonia removal from NASA's advanced life support wastewater system to establish long-term human presence in space. Natural zeolites are also produced for Pb^{2+}, and Cd^{2+} removal from wastewater. In the nutrition and health field, clinoptilolite appears to be stable in the gastrointestinal tract and reduces ammonia toxicity in pigs and sheep. Pigs, chickens and turkeys are protected from mycotoxins in contaminated grains. In general, addition of 1 to 5 wt % to the diet of animals has been shown to improve growth and feed utilization and to reduce incidence and severity of diarrhea in pigs, cattle, sheep, and chickens. Ag-exchanged clinoptilolite eliminates the microorganisms *E. coli* and *S. faecalis* from water after 2 h of contact time. Clinoptilolite application is not restricted to animals but an anti-diarrheic drug (ENTEREX) has also been developed for humans (Armbruster, 2001).

The most important step in the specific application of zeolites is the clarification of the fundamental processes and basic interactions taking place in the channel and cage systems related to ions and molecules accessing the zeolite cavity system. If these processes are understood, new application fields will be possible and existing fields will be deepened and widened if zeolites with the properties needed are available (Ghobarkar et al, 1999).

CHAPTER 3

EXPERIMENTAL

3.1. Preparation of the Natural Zeolitic Tuff

The natural zeolite tuff obtained from Gordes-Fındıcak (Manisa, Turkey) region in 3 m depth from the surface was crushed and sieved to the particle size range of 850 – 2000 μm, washed with distilled water for 2 hours at 60 ^{o}C to remove the soluble salts. Approximately 2.5 wt % of the as-received zeolitic tuff (NCU) was removed as impurities. The washed zeolite (NCW) was dried in a vacuum oven at 160 ^{o}C for 24 h before employing in the acid treatment studies.

3.2. Acid Treatment of the Natural Zeolitic Tuff

Five grams of zeolites (NCW) were put into 100 ml of HCl, H_2SO_4, HNO_3, and H_3PO_4 solutions for acid treatments. The acid treatment was carried out in a shaker (GFL 1092) with a shaking rate of 200 rpm at 60 ^{o}C for 6 and 3 hours, then the solutions were filtered with blue band filter paper. For the 6 hours treatment, the concentrations of the acid solutions used to obtain the zeolites; **C1-6h, C3-6h, C5-6h,** and **C10-6h** were for 1, 3, 5 and 10 M HCl, **N1**, **N2, N5** were for 1, 2, and 5 M HNO_3, **S1** and **S2** were for 1 and 2 M H_2SO_4, and **P1** for 1.1 M H_3PO_4 treated zeolites respectively. For the 3 hours treatment, the concentrations of the acid solutions used to obtain the zeolites; **C3-3h** and **C10-3h** were for 3 and 10 M HCl treated zeolites respectively.

Acid treated samples were carefully washed with double-distilled water in order to remove the chloride, sulfate, nitrate, and phosphate ions from the zeolite structure. For the zeolites treated with HCl, $AgNO_3$ solution was used to control the AgCl precipitation. The control procedure was done with phenoldisulfonic acid for the nitrate ion determination and with barium chloride and conditioning reactive (TSE, UDK 662.6: 543, 1984) for the sulfate ion determination.

3.3. Characterization of the Natural Zeolitic Tuff

Chemical composition of the original washed zeolite (NCW) was obtained by the fusion dissolution technique using $Li_2B_4O_7$. 100 mg sample of the zeolite was combined with 0.7 g of lithiumtetraborate. The dry-powder mixture was then placed in a platinum crucible and fused in an oven at 1000 ^oC for approximately 1h. After cooling it was dissolved in hot aqueous 100 ml of 1.6 M HNO_3 solution and brought to 5 % HNO_3 concentration in 250 ml by adding deionized water. This solution was then presented to the Inductively Coupled Plasma Atomic Emission spectroscopy (ICP 96, Varian). The resulting elemental concentrations were then translated to their oxide forms to represent the final composition. The fused sample was also sent to EDX (EDAX) coupled to a Scanning Electron Microscope (SEM, Philips XL 30S) in order to compare the results with the results of the bulk composition obtained from the ICP measurement.

The filtered acidic solutions of the acid treated zeolites were also analysed by using the ICP instrument. The chemical compositions of the acid treated zeolites were then calculated from the difference between the amounts of ions in the original washed zeolite (NCW) and the filtered acidic solutions.

Mineralogy of the original zeolitic tuff and the crystallinities of the acid treated zeolites were determined by powder X-ray diffraction (X-Pert Pro Diffractometer) using CuK_α radiation. (λ =1.54051 Å) at 45 kV and 40 mA with a step size of 0.02^o 2θ. The analyses were performed in the 5-40^o 2θ range.

For texture structure of the zeolites, the nitrogen adsorption isotherms were obtained at liquid nitrogen temperature (77 K), using an ASAP 2010 apparatus (Micromeritics). Prior to the determination of the adsorption isotherms, the samples were degassed for 24h at 350 ^oC.

Thermal properties of the zeolites were analysed by thermobalance (Schimadzu TGA-51 thermobalance) and differential thermal analyzer (Schimadzu DTA-50). Zeolites (~10 mg) were scanned between 30 and 1000 ^oC with a heating

rate of 10 ^{o}C/min. All analyses were made using dynamic (40 ml/min) nitrogen atmosphere.

Scanning Electron Microscope (Philips XL 30S) was used to take the microphotographs of the zeolite crystals. The infrared spectra of the samples were recorded at room temperature by using KBr (1/50) pellet technique in the Shimadzu FTIR-8601 device. The spectrum between 400 - 4500 cm^{-1} wavelengths were analysed.

For the heat capacities of the zeolites at 26 ^{o}C, Setaram Microcalorimeter (C80) was used between 20-30 ^{o}C with an increment rate of 0.1 ^{o}C /min. Alumina (Al_2O_3) powder with a heat capacity of 0.1756 cal/Kgr at 26 ^{o}C was used as the reference.

CHAPTER 4

RESULTS & DISCUSSION

4.1. Identification and Characterization of the Natural Zeolitic Tuff

Heulandite and clinoptilolite are identical in structure and distinguishing them had been a subject of confusion for many years. In the study of Mumpton (1960), a conclusion was made that, with clear examination of X-ray, chemical, optical and thermal properties, these two minerals can be distinguished from eachother. Goryainov et al, (1995) also agreed that these two zeolites commonly differ by thermal behaviour and chemical composition.

Natural zeolitic tuff used in this study was carefully characterized and its characteristics (chemical, optical, x-ray, spectroscopic and thermal) were compared with +90 % pure, clinoptilolite, IDA, (10×20 mesh, # 27031 Castle Creek, Idaho) kindly supplied by Mumpton F.

4.1.1 Chemical Analysis of the Natural Zeolitic Tuff

The chemical compositions of the zeolites measured by using ICP and EDX instruments are shown in Table 4.1. The chemical compositions of the fused and unfused NCW zeolite measured by the EDX analysis showed that, although the silicon and aluminium contents seemed to be similar, the exchangeable cation amounts were different from each other. Also iron was not detected for the fused NCW sample with the EDX analysis since iron has the highest molecular weight among those cations and may be precipitated to the bottom during fusion and therefore could not be detected by the surface EDX analysis. Comparison of the techniques for the fused NCW sample showed that, except for aluminium, the cation contents were found not to be similar. Therefore it may be evaluated that although some inconsistencies in some of the cation contents exist for the two different techniques, silicon and aluminium contents were found to be

unaffected considerably. Concentration difference is probably due to surface enrichment during fusion, and EDX-SEM is sensitive to surface as compared to ICP.

The chemical compositions of the heulandite – clinoptilolite series is characterized by remarkable changes in the Si/Al ratio as well as in the composition of exchangeable cations. Numerous statistical treatments of published chemical analyses have revealed clear correlations; as a rule, low-silica members of the heulandite-clinoptilolite group are enriched with calcium and often contain Ba and Sr, whereas high silica members are enriched with potassium, sodium and magnesium. Of the alkali metal cations, sodium is more characteristic for heulandite and potassium for clinoptilolite (Tsitsishvili et al, 1992). In the study of Esenli (1993), after the chemical analyses of zeolitic tuffs from Gördes region, it was found that, K_2O was detected in the heighest wt % among the other exchangeable cations for clinoptilolite samples, and CaO for heulandite samples. In the ICP analysis of the fused NCW zeolite, EDX analysis of unfused NCW, and the EDX analysis of IDA zeolite, potassium was detected more than the other exchangeable cations (Table 4.1).

Table 4.1. Chemical compositions of the washed zeolitic tuff (NCW) and IDA

Oxides (wt %)	NCW [a] (fused)	NCW [b] (fused)	NCW [b] (unfused)	IDA [b] (unfused)
Al_2O_3	14.1	14.5	15.06	14.05
SiO_2	64.2	62.3	62.4	67.1
MgO	1.8	4.2	1.6	1.4
Na_2O	1.7	3.1	1.6	1.9
K_2O	5.3	3.0	4.3	2.5
CaO	1.0	2.6	4.2	-
Fe_2O_3	1.8	-	0.8	-
H_2O [c]	10.3	10.3	10.3	13

[a] Measured by ICP analysis
[b] Measured by EDX analysis (average of 2 grains were taken)
[c] Measured by TGA analysis

It was stated that there are three (not two) minerals concerning the heulandite-clinoptilolite group: heulandite (I), intermediate species (II), and clinoptilolite (III) (Drebushchak et al, 2000). Instead of “intermediate species”, high silica

heulandite and low silica clinoptilolite was used by Tsitsishvili et al, (1992). According to tradition high silica clinoptilolite is called traditionally simply clinoptilolite, and low silica clinoptilolite known as Ca-clinoptilolite. According to Drebushchak et al, (2000) two parameters are necessary to identify what mineral the sample under question refers to. These are Si/Al and $\Sigma M^{++}/\Sigma M^{+}$ ratios. Here ΣM^{++} is the sum of the divalent cations and ΣM^{+} is the sum of the univalent cations. The subcommittee on zeolites of the International Mineralogical Association recommends distinguishing two species as heulandite (Si/Al <4) and clinoptilolite (Si/Al >4) by considering the framework cations. But in this study, instead of the framework compositions, bulk compositions (consisting of both framework and extraframework cations) of the zeolite samples were calculated. Therefore $\Sigma M^{++}/\Sigma M^{+}$ ratio will guide us to find out the mineral in question. The ratio of the sum of the divalent cations (Ca, Mg) to the sum of the univalent cations (Na, K) was found as 0.33 for NCW sample and 0.23 for IDA zeolite. According to Table 4.2, NCW and IDA zeolites can be identified as clinoptilolite for their $\Sigma M^{++}/\Sigma M^{+}$ ratios.

Table 4.2. Identification of the clinoptilolite and heulandite minerals (Drebushchak et al., 2000)

Mineral Classification	[a]Si/Al	[a]$\Sigma M^{++}/\Sigma M^{+}$	[b]Si/Al	[b]$\Sigma M^{++}/\Sigma M^{+}$
Heulandite	2.90-3.52	10.31-1.61	2.85-3.73	3.69-0.88
Intermediate	3.57-4.31	2.20-0.43	3.45-4.35	2.06-0.73
Clinoptilolite	4.12-5.10	0.60-0.09	5.10-5.20	0.37-0.16

[a] Classification by Boles (1972)
[b] Classification by Alietti (1972)

4.1.2. X-ray Diffraction and Optical Analysis of the Natural Zeolitic Tuff

The main characteristic peaks of the clinoptilolite – heulandite crystal phases in the X-ray diffraction patterns are at 2θ values of 9.84^{o} and 22.45^{o} which correspond to (020) and (004) planes respectively. According to Mumpton, (1960) there are distinct differences in the literature concerning the intensities of the XRD peaks of heulandite and clinoptilolite. The XRD peaks of clinoptilolite are found to be much stronger and somewhat broader than those of heulandite by Mumpton, (1960). Also it was noted by Mumpton, (1960) that many of the peaks present in clınoptilolite are absent in heulandite and the (020) reflection of heulandite was always far more intense than the remaining lines of the pattern, while this same reflection in XRD pattern of clinoptilolite was in many samples, exceeded in intensity by the (004) peak. Mumpton (1960) made a conclusion according to the XRD results of both heulandite and clinoptilolite that, the many differences between diffractometer tracings of both minerals have proved quite adequate identification and differentiation between these two zeolites. Figure 4.1 shows the comparison of the XRD patterns of the original washed (NCW) and +90 % pure IDA clinoptilolite.

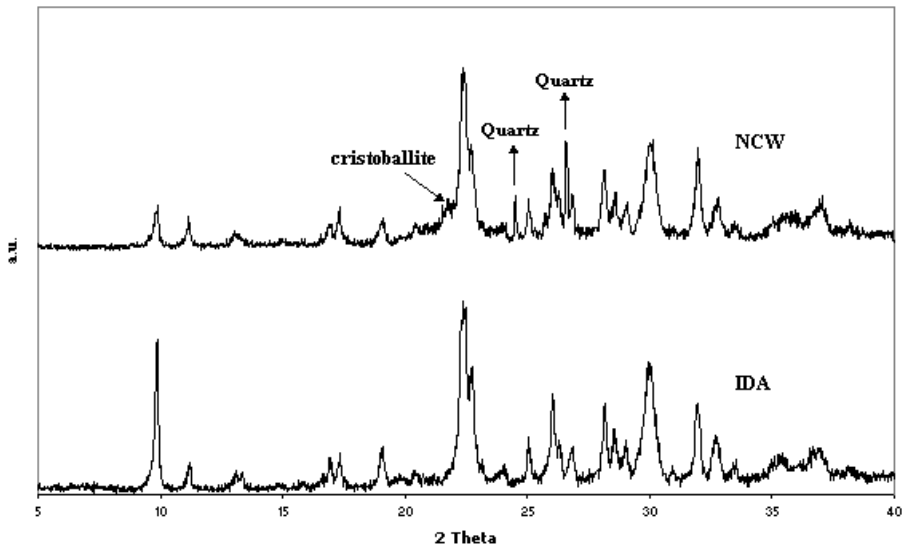

Figure 4.1. X-ray diffraction patterns of the washed original zeolite (NCW) and + 90 % pure clinoptilolite (IDA)

XRD pattern of IDA zeolite showed that all the peaks were matched with the clinoptilolite-heulandite peaks, and no other crystal phases were detected in its XRD pattern. But in the XRD pattern of the NCW sample, except for the clinoptilolite-heulandite peaks, low cristoballite and quartz peaks were also detected. It is clear for both zeolites that, the (004) peak intensities exceeded those of (020) indicating that zeolites contain clinoptilolite, not heulandite. If the peak intensities of IDA and NCW are examined, although the peaks at $2\theta = 22.45^{o}$ seems to be at same height, peak at $2\theta = 9.84^{o}$ of IDA zeolite is found to be much higher than that of NCW. This finding may be due to the preferred orientation of the crystals of the IDA zeolite in the (020) plane. Qualitatively but not quantitatively, it may be said that IDA zeolite has better crystallinity and has higher clinoptilolite content than NCW.

The cleanless and brightness of the IDA crystals is easily seen in Figure 4.2, while in the SEM microphotographs of NCW, some impurities are seen on the zeolite (Figure 4.3). SEM microphotographs showed the classical morphology of individual tabular crystals (coffin shaped). The crystals appear mostly in cavities and the majority of the clinoptilolite crystals in the washed sample were anhedral (Figure 4.4).

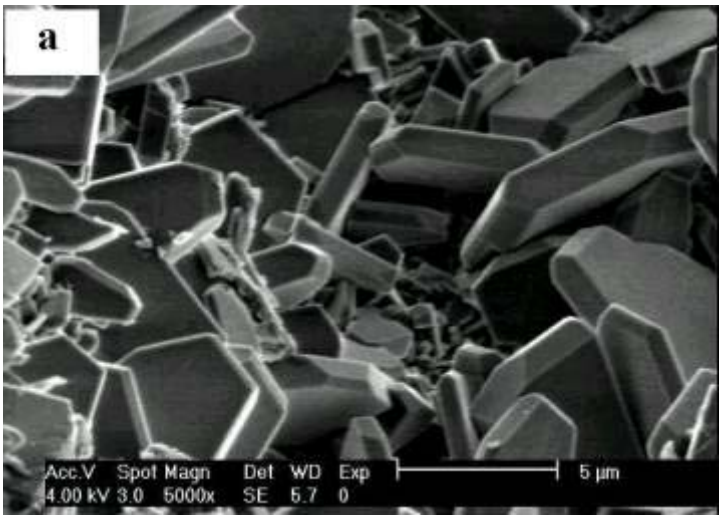

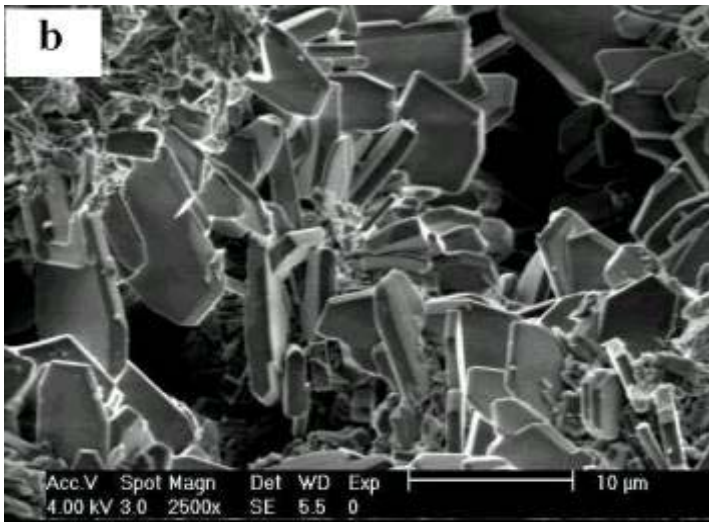

Figure 4.2. SEM microphotographs of + 90 % pure clinoptilolite (IDA)

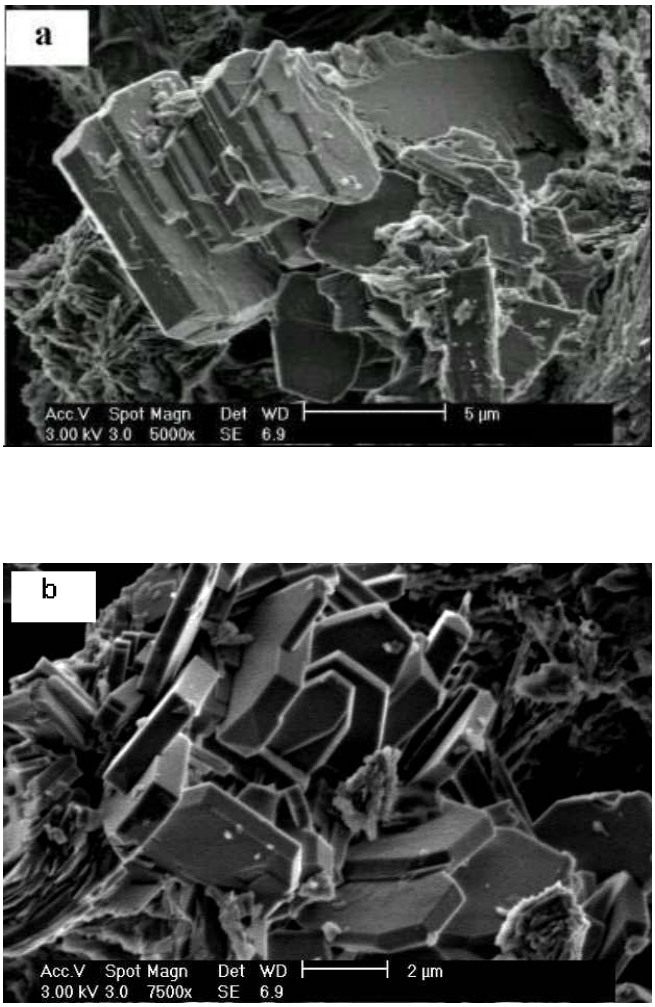

Figure 4.3. SEM microphotographs of washed zeolitic tuff (NCW)

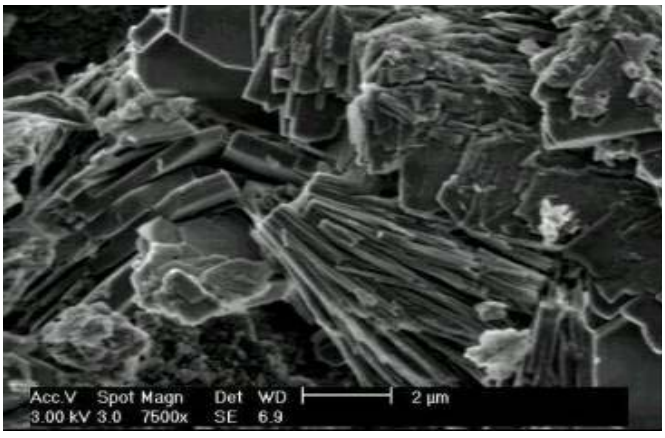

Figure 4.4. SEM microphotograph of washed zeolitic tuff (anhedral morphology)

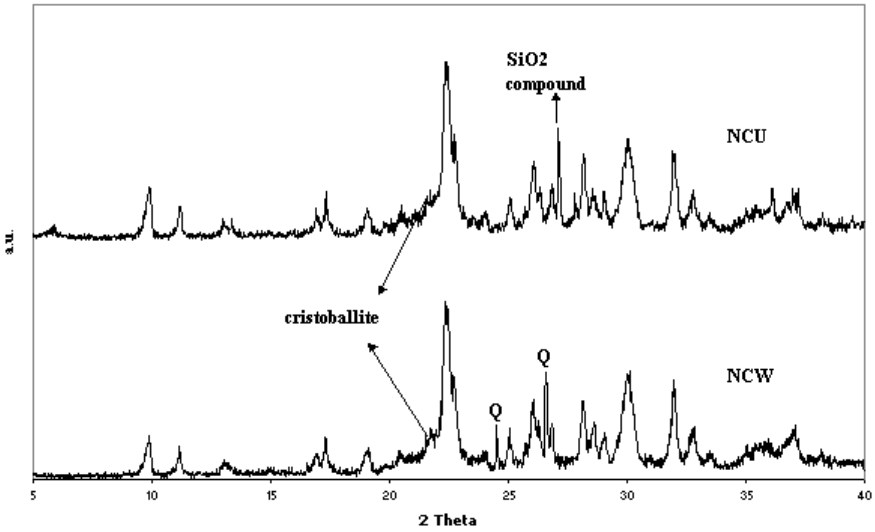

Figure 4.5. X-ray diffraction patterns of the as - received (NCU) and washed zeolite (NCW) (Q is for quartz)

Figure 4.5 compares the XRD patterns of the as-received (NCU) and washed natural zeolites (NCW). Except for the peaks that are attributed to clinoptilolite, low cristoballite, quartz and some other SiO_2 compound were observed in the samples. Quartz did not come into structure by washing, but it was not detected in the analyzed NCU sample, since the zeolitic tuff was heteregenous. The two XRD patterns showed similarities in the 2θ values of the peaks and the peak intensities. The water-soluble impurities that were not detected around the zeolite crystals of the original washed sample (Figure 4.3), are clearly seen from the SEM microphotograph of the as-received natural zeolitic tuff (Figure 4.6).

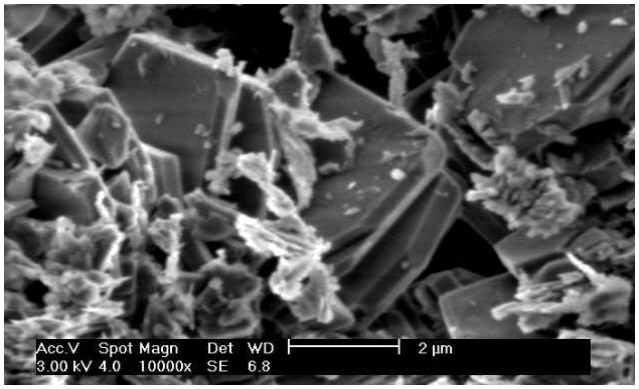

Figure 4.6. SEM microphotograph of the as - received zeolitic tuff (NCU)

4.1.3. IR Analysis of the Natural Zeolitic Tuff

Infrared spectroscopy has been used successfully for studying zeolite structure and properties (Goryainov et al, 1995). The region in the infrared spectrum between 1200 and 400 cm^{-1} has been used as a structural fingerprint for the zeolites (Zhao et al, 1998). Assymetrical stretching vibrations of internal tetrahedra linkages due to Si-O-Al bondings in the framework (1074 cm^{-1}), internal tetrahedra T-O bending (470cm^{-1}), external tetrahedra double ring due to O-T-O bending (610 cm^{-1}), the T-O asymmetric stretching vibration of free tetrahedra (1202-1212 cm^{-1}) and external tetrahedral linkage symmetric streching (795 cm^{-1}) are the characteristics for the clinoptilolite mineral. It turned out by comparison of spectral and structural features that the internal vibrations are largely structure insensitive, whereas the position of the bands due to vibrations of external linkages are often structure sensitive (Weitkamp and Puppe, 1999). Absorption bands of 610 and 1212 cm^{-1} were selected as the representative bands for the quantitative determination of clinoptilolite content in tuffaceous rocks in the study of Goryainov et al, (1995). Figure 4.7 shows the IR patterns of IDA and NCW. In order to see the relative change of the external tetrahedra double ring vibration with respect to the other vibrations, peak intensity ratios were measured and found that although the peak intensity ratios of 607 cm^{-1}/1066 $cm^{-1}$and 607 cm^{-1}/460 $^{-1}$cm are the same (0.16 and 0.54) for IDA and NCW respectively, the ratio of 607 cm^{-1}/795 cm^{-1} of IDA was measured (2.65) higher than that of NCW (2.16), indicating that IDA zeolite has more clinoptilolite content than NCW zeolite.

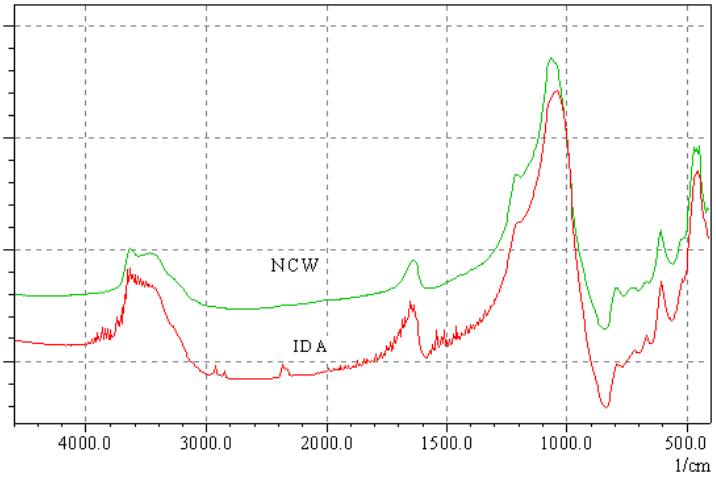

Figure 4.7. IR patterns of washed original zeolite (NCW) and + 90% pure clinoptilolite IDA (absorbance in a.u. vs wavenumber)

4.1.4. Thermal Analysis of the Natural Zeolitic Tuff

According to Tsitsishvili et al, (1992) typical heulandite and clinoptilolite are clearly distinguished by their DTA curves due to the fact that the intensities and the temperature of the maxima of DTA curves depend both upon the cations and the Si/Al ratio. Water is released from heulandite in two stages with maxima at 210 and 340 ^{o}C. X- ray studies of the heated samples show that splitting of the endothermic peak is associated with structural rearrangement of the sample; metaheulandite B is formed. On the DTA curves of clinoptilolite, only one endothermic effect is recorded with maxima at 140 ^{o}C (Tsitsishvili et al, 1992). According to Mumpton (1960), in heulandites, sharp steepening of the weight loss curve happened around 250 ^{o}C due to the transformation of heulandite to heulandite B, but in clinoptilolites, no break in the weight loss curve was observed. Similarly, in the DTA patterns of heulandite, an additional very sharp endotherm was noted at about 300 ^{o}C caused by heulandite B formation. But in the DTA patterns of clinoptilolite no transitions or reactions were observed up to 750 ^{o}C. Then the collapse of the structure was noted. Both authors have data in common, as the transformation of heulandite to another phase at around 250-340 ^{o}C and no change of phase for clinoptilolite at those temperatures.

Figure 4.8 displays the XRD patterns of the original natural zeolite and its overnight heated (400 ^{o}C) form. It is obvious that no structural rearrangement of the sample has occurred by heating to 400 ^{o}C, proving that the zeolite is exactly clinoptilolite.

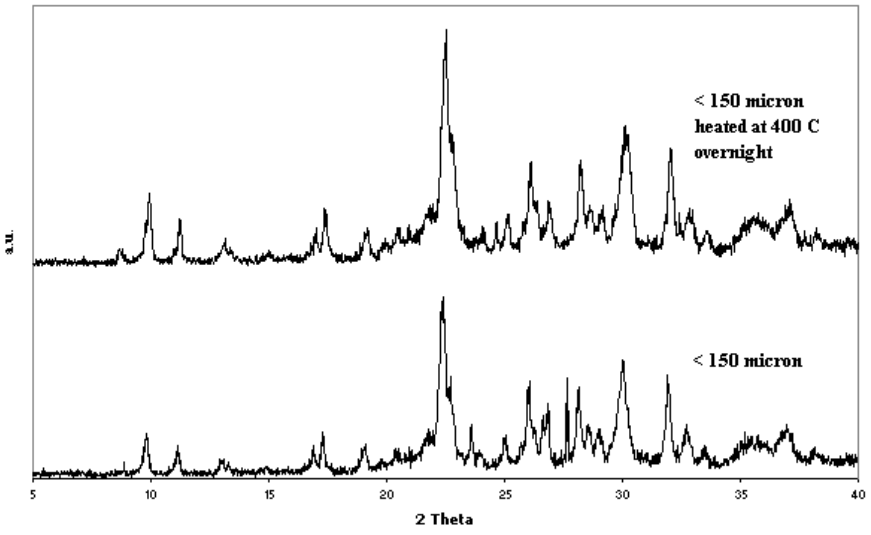

Figure 4.8. X-ray diffraction patterns of the original natural zeolite and its overnight heated (400 ^{o}C) form

Figures 4.9 and 4.10 display the TGA and DTA curves of the original zeolites. No additional sharp endotherm in the DTA curve or any steepening in the weight loss curves at around 250-340 ^{o}C was observed. Due to the destruction of the crystal structure, an exotherm was observed for NCW sample at around 950 ^{o}C. Thermal data proves that, the zeolites used in this study are clinoptilolite.

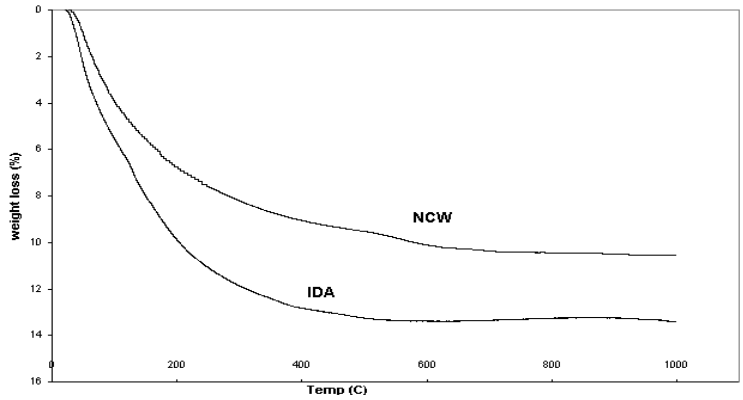

Figure 4.9. TGA curves of washed original zeolite (NCW) and +90 % pure clinoptilolite (IDA)

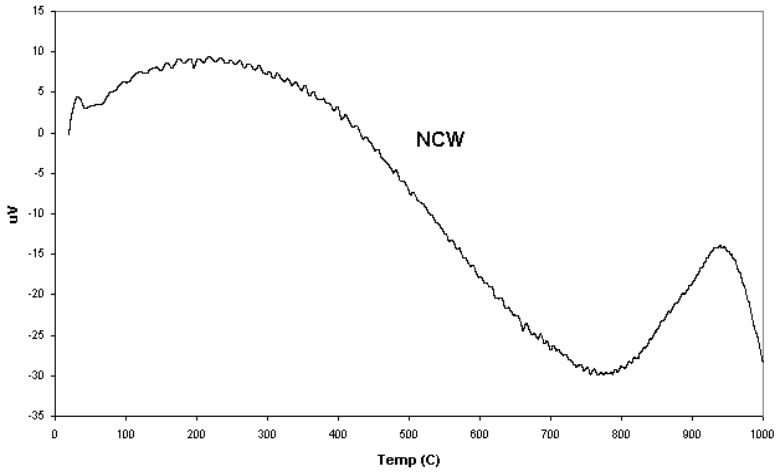

Figure 4.10. DTA curve of washed original zeolite (NCW)

4.2. Acid Treatment Studies

In this study, the effect of HCl, H_2SO_4, H_3PO_4 and HNO_3 in aqueous media on modification of original natural zeolite, clinoptilolite, was examined. Firstly the comparison of the acids is introduced. Depending on the nature of the acid, some or all of its molecules may ionize when the acid is dissolved in water. The strength of an acid is determined by the extent to which its molecules undergo ionization. Ionization rate depends on a number of factors, such as the properties of the solvent, the temperature, and the molecular structure of the acid. If the acids are compared to each other, some variables can be eliminated by considering their properties in the same solvent and the same temperature. So the molecular structure of the acids, in other words the bond dissociation

energies of the acid molecules become the main parameter determining the ionization rates. The bonds with high dissociation energies are less easily ionized than weaker ones (Chang, 1994). The bond dissociation energy of H-Cl (431.9 kJ/mol) is smaller than that of H-O (460 kJ/mol) of the other acids in consideration, so HCl is said to be the strongest acid used in this study. HCl and HNO_3 are monoprotic acids; that is each unit of the acid yields one H^+ ion, but H_2SO_4 is a diprotic acid because each unit of the acid yields two H^+ ions, in two separate steps. These three acids are all strong acids because they are strong electrolytes, so they are completely ionized in solution. H_3PO_4 is a tripotic acid that yields three H^+ ions, in three separate steps, and all the three species (H_3PO_4, $H_2PO_4^-$, and HPO_4^{2-}) that are formed in the ionization are weak acids. So H_3PO_4 is the weakest acid used in this study.Weight percentages of the cations for the washed (NCW), IDA and the acid treated zeolites are shown in Table 4.3. As the acid concentrations increased, it is seen that more aluminums and other cations were removed from the zeolite structures. Some incoherent results for some cations are due to the usage of different analysis techniques. Si/Al ratio of the original zeolite was found as 4.04 and this ratio changed from 5.25 to 5.35 with H_2SO_4, from 5.91 to 6.39 with HNO_3 and from 5.25 to 10.8 with HCl treatments, and changed to 5.01 with H_3PO_4 treatment. It is clear that HCl treatment affected the Si/Al ratios the most. HNO_3 treatment seemed to be more effective than H_2SO_4 treatment, and H_3PO_4 treatment was found to be the least effective of all.

Table 4.3. Cations (wt %) for washed and acid treated zeolites

Cations	NCW	S1	S2	C1-6h	C3- 6h[a]	C5-6h	C10-6h[a]	C3- 3h[a]	C10-3h[a]	N1	N2[a]	N5	P1[a]	IDA
Al	15. 9	14	13. 8	13. 9	11	9. 4	7. 8	12. 6	9. 4	12. 7	12. 6	11. 9	14	16.4
Ca	2. 9	0. 3	0. 1	0. 3	1. 5	0. 02	1. 2	1. 6	1. 1	0. 1	1. 8	0. 05	2.5	-
Fe	2. 5	0. 6	0. 5	1. 2	2. 7	0. 9	2. 4	2. 9	2. 9	0. 8	1. 8	0. 9	3.1	-
K	9. 9	8. 8	8. 8	9. 3	1. 8	8. 2	1. 4	1. 9	1. 3	8. 5	2. 8	8. 4	6.0	5.1
Mg	1. 4	0. 7	0. 7	0. 8	1. 5	0. 5	1. 5	1. 9	1. 7	0. 7	1. 7	0. 7	2.0	1.8
Na	3. 2	2	2. 1	1. 5	1. 4	1. 9	1. 5	1. 7	1. 4	2. 1	1. 4	1. 9	1. 8	2.9
Si	64. 2	73. 6	73. 9	73	80	79	84	76. 6	82	75. 1	78. 4	76. 1	70. 2	73.9
Si/Al	4. 04	5. 25	5. 35	5. 25	7. 3	8. 4	10. 8	6. 08	8. 7	5. 91	6. 18	6. 39	5. 01	4.5

[a] Measured by EDX analysis (average of 8 different grains were taken)

4.3. X-Ray Diffraction Analysis of the Acid Treated Zeolites

Figures 4.11 to 4.15 display the XRD patterns of the acid treated zeolites. XRD patterns of the H_2SO_4 and HNO_3 treated samples (Figures 4.11 and 4.12) showed that, as the acid concentrations increased, intensities of the characteristic peaks decreased, meaning a loss in the crystallinities of the zeolites and no other extra peaks of any sulfate or nitrate compounds were observed. XRD results of H_2SO_4 and HNO_3 treated samples confirmed the Si/Al ratios indicating that, as the acid concentrations were increased, more framework aluminums were affected leading to more crystallinity loss. From the XRD data of the HCl treated zeolites for 6h (Figure 4.13), it is clear that, with 1 M and 10 M HCl treatments, the characteristic peaks almost disappeared which means that the crystal structures were collapsed and the amorph phases were generated. Although 3 M HCl treatment affected the crystal structure, 5 M HCl treatment seemed to be the least effective one preserving the crystal structure. Decreases in the Al concentrations and partial surface amorphization due to the attack of 1 M and 2 M HCl was also mentioned for clinoptilolite and heulandite samples by Armbruster, (2001). In our study, although the amorphization of the zeolite with 1M HCl treatment was observed, the Si/Al ratio of this zeolite was found to be low (5.25) which may be explained by the formation of the octahedral aluminium complexes on the zeolite surface caused by the migration of the tetrahedral aluminas, and the inability of those big dimensional complexes migrating out of the zeolite, also detected by Giudici et al (2000). Effect of the chloride ions and concentrations on alumina dissolution of clinoptilolite via the formation of innersphere complexes with surface groups was deeply studied by Doula et al, (2002), and in their study it was found that, occurrence of chloride ions not only forms the Al-Cl bonds that are highly polarized due to the different electronegativities and can easily be broken, increasing the Al dissolution, but also may stabilize the surface-OH_2^+ groups via the formation of outersphere complexes of the type surface-OH_2^+...Cl^- inhibiting Al dissolution. Moreover, the increase in Cl^- concentration favors the formation of aquatic complexes between Cl^- and Al^{3+} (e.g., $AlCl_4^-$) inhibiting also the hydrolysis of Al^{3+} and

consequently the production of H^+. Therefore one may conclude that the increasing presence of Cl^- in solution has positive as well as negative effects on Al dissolution. In the light of that information about the behaviour of Cl^- ions, it may be evaluated that 3 and 5 M HCl treatments, due to their high Cl^- concentrations, were not as successful as 1 M HCl treatment on attacking to the framework aluminas, experiencing the negative effects of Cl^- ions in solution, and mostly attacked to the extraframework cations, but 3 M HCl treatment resulting better in Al dissolution and forming aluminium complexes on the zeolite surface. Therefore the Si/Al ratio of 5 M HCl treated zeolite is found (8.4) higher than that of 3 M HCl (7.3). In the case of 1 M HCl treatment, experiencing the positive effects of Cl^- ions in solution, as mentioned above, formation of the octahedral aluminium complexes on the zeolite surface caused by the migration of the tetrahedral aluminas, and the inabilities of those big dimensional complexes migrating out of the zeolite explains the great framework loss, but with a low Si/Al ratio (5.25). 10 M HCl treatments, experiencing both the negative and positive effects of Cl^- ions in solution, affected the framework structure so strongly that the crystal structure collapsed. Probably with 10 M HCl treatments, all the possible inhibiting effects played role as in the 3 and 5 M HCl treatments, but the solution pH is so low that, they could not prevent the framework from dissolution. It is probable that, the formed big-dimensional aluminium complexes due to framework Al dissolution has migrated out of the zeolite structure through the strongly destroyed pore openings, and therefore the Si/Al ratios were measured high for 10 M HCl treatments.

3 M HCl (6 and 3 hours) treated samples resulted with nearly the same XRD patterns and the peak intensities, but it seems that 6h treatment lowered percentage of crystal phase slightly more than 3h treatment (Figures 4.13 and 4.14). If the 10 M HCl treated zeolites (3 and 6 hours) are compared to each other, unexpectedly C10-6h sample displayed slightly visible peaks, whereas C10-3h sample gave a totally amorphous XRD pattern.

As expected, H_3PO_4 treatment did not affect the crystal structure so much for being the weakest acid of all (Figure 4.15). Peak intensities decreased slightly

and no other extra peaks for any phosphate compounds were detected in the pattern. The ineffectiveness of H_3PO_4 treatment on clinoptilolite was also stated by Pozas et al. (1996). However significant loss of phillipsite zeolite was noted by using 1 N, 2 N and 3 N H_3PO_4 (Notario et al, 1995).

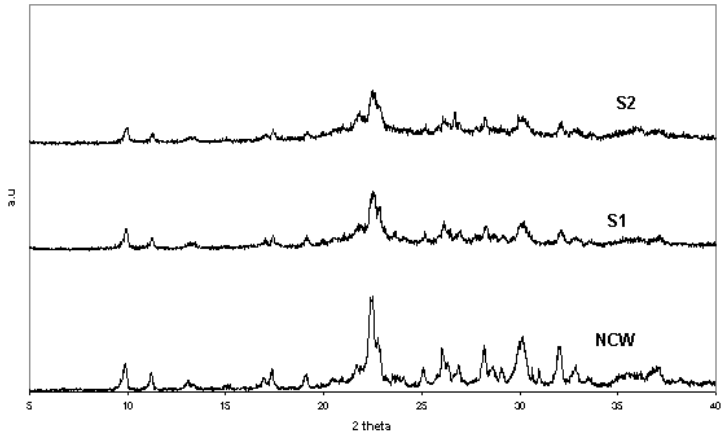

Figure 4.11. X-ray diffraction patterns of the H_2SO_4 treated zeolites and NCW

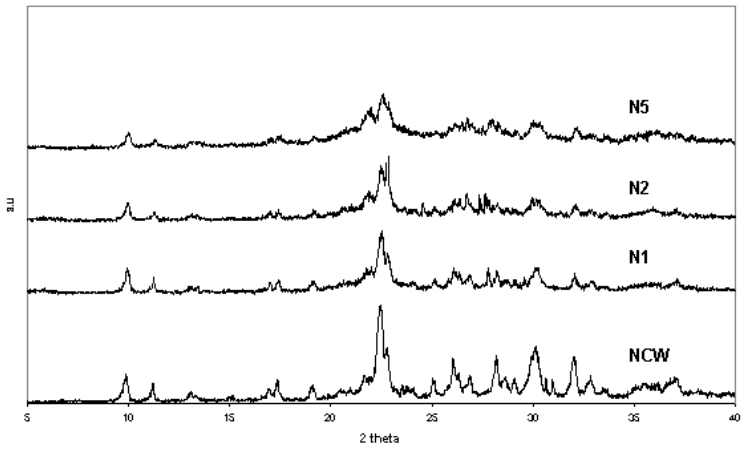

Figure 4.12. X-ray diffraction patterns of the HNO_3 treated zeolites and NCW

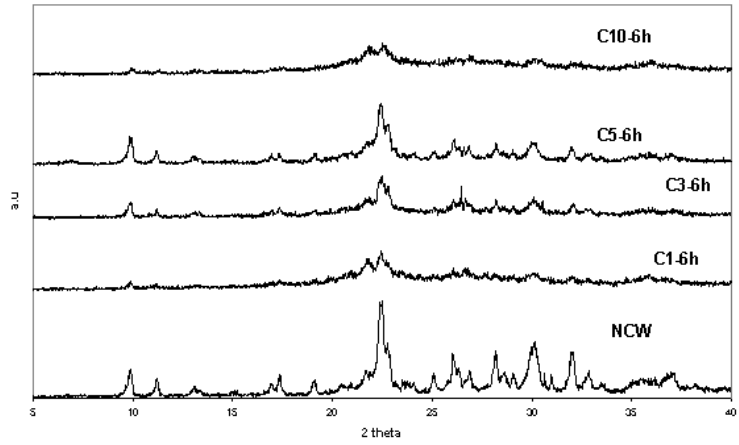

Figure 4.13. X-ray diffraction patterns of the HCl treated zeolites (6h) and NCW

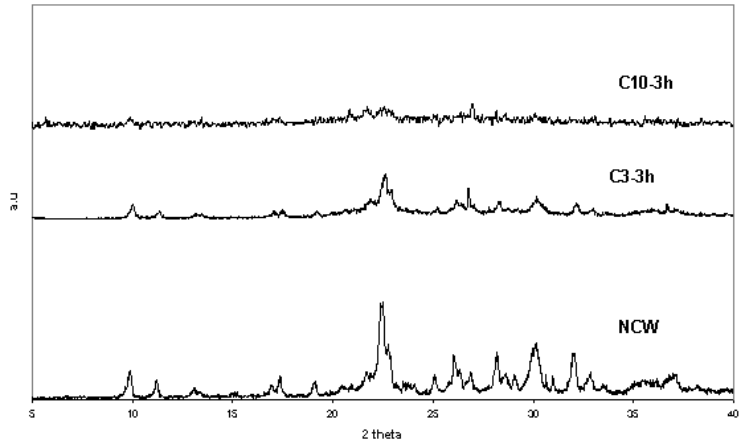

Figure 4.14. X-ray diffraction patterns of the HCl treated zeolites (3h) and NCW

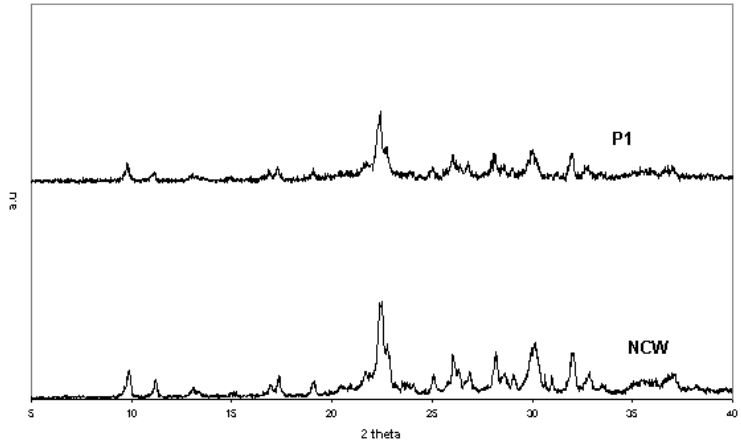

Figure 4.15. X-ray diffraction patterns of 1.1M H_3PO_4 treated zeolite and NCW

4.4. Adsorption Properties of the Original and the Acid Treated Zeolites

The adsorption isotherms of the original and the acid treated zeolites are given in Figures 4.16 to 4.20. The isotherms of the acid treated zeolites exhibit type I isotherms in the BDDT classification.

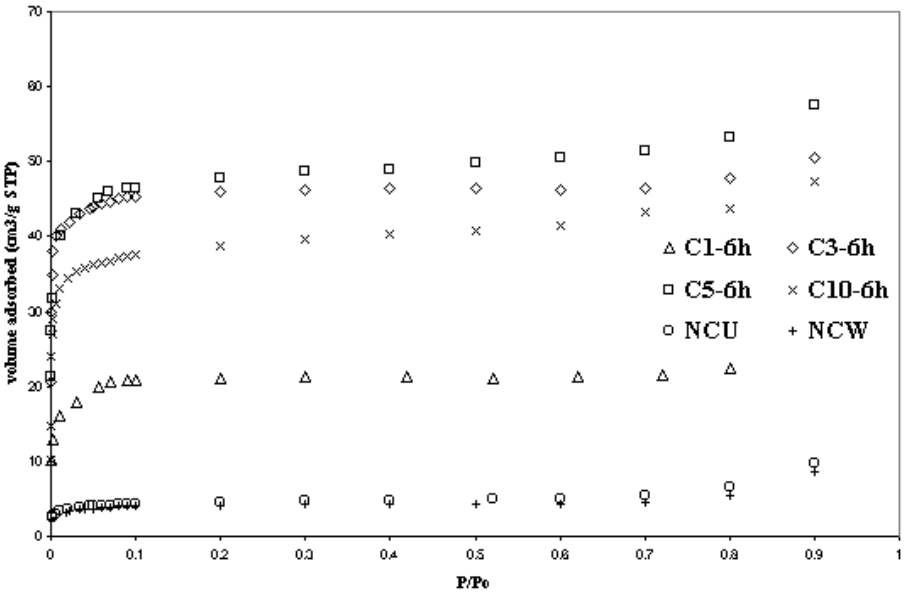

Figure 4.16. N_2 Isotherms of HCl treated (6h) and original zeolites

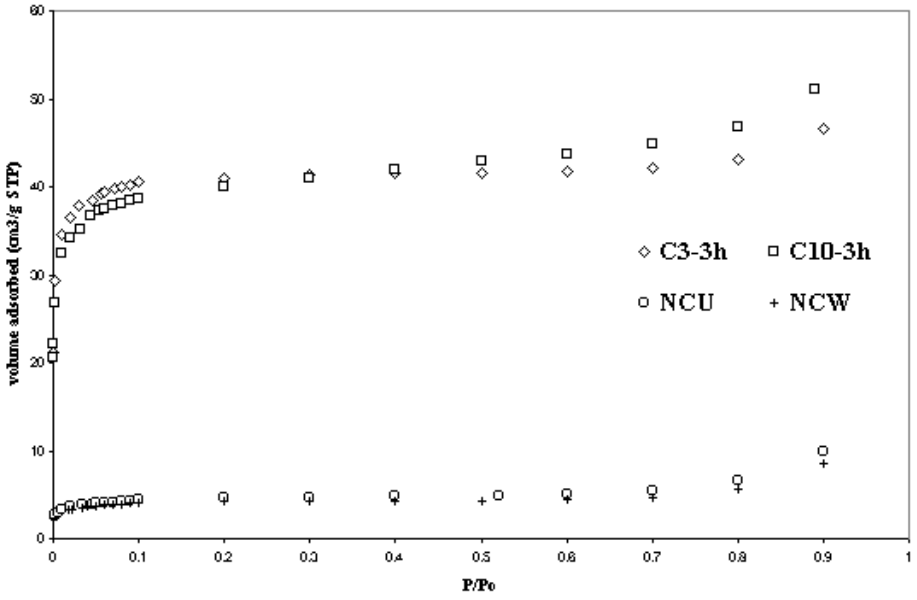

Figure 4.17. N_2 Isotherms of HCl treated (3h) and original zeolites

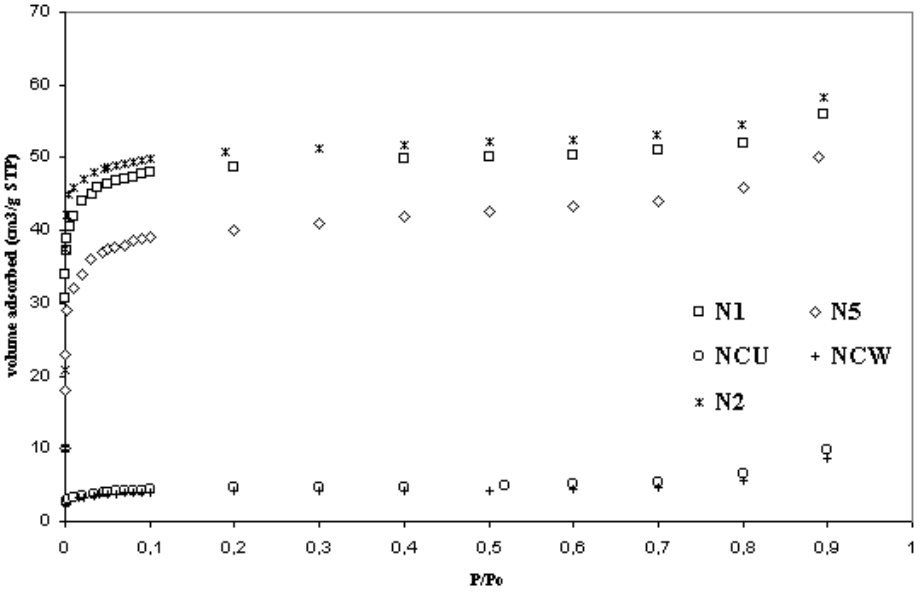

Figure 4.18. N_2 Isotherms of HNO_3 treated and original zeolites

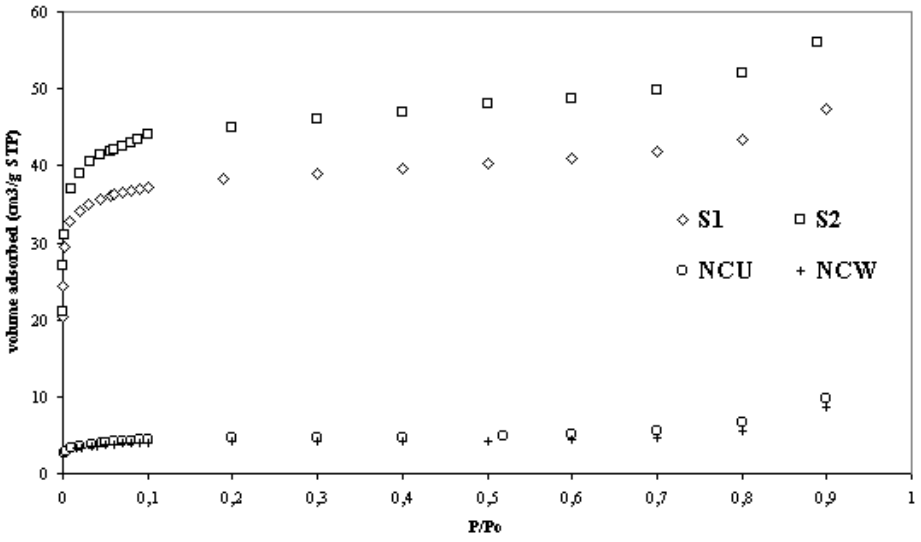

Figure 4.19. N_2 Isotherms of H_2SO_4 treated and original zeolites

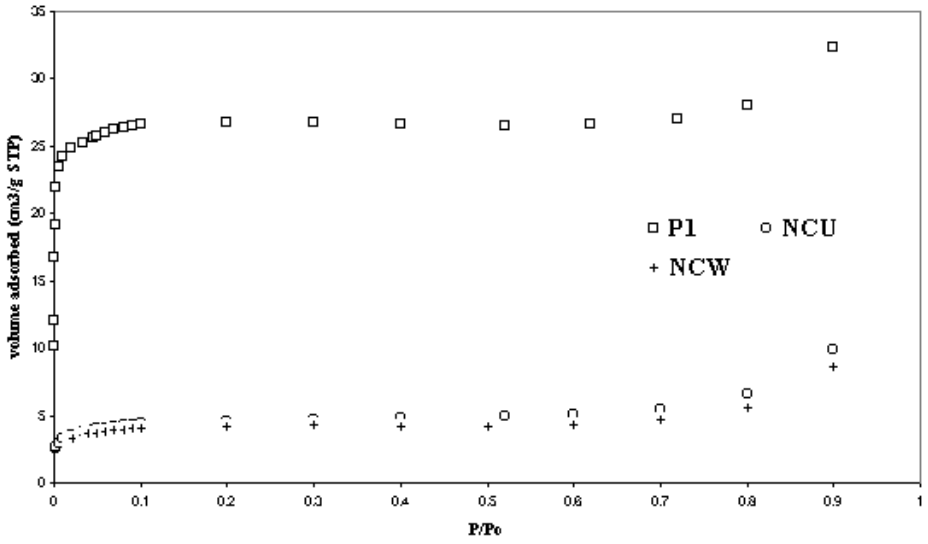

Figure 4.20. N_2 Isotherms of H_3PO_4 treated and original zeolites

In this study, the Dubinin-Astakhov, Horwart Kawazoe, t- method and Langmuir equations were used for the evaluation of micro and mesostructural parameters of zeolites.

Monolayer capacity, n_m was calculated from the Langmuir model, equation:

$$p/n = 1/n_m b + p/n_m \quad (4.1)$$

where n is the specific amount of gas adsorbed at the equilibrium pressure p, to determine the specific surface area, A, of the zeolite from the equation:

$$A = n_m a_m L \quad (4.2)$$

where a_m : average area occupied by a molecule of adsorbate in the completed monolayer (taken as 16.2 $Å^2$ for nitrogen), L : Avagadro constant.

Micropore volumes, V_{micro} and external surface areas, A_{ext} were calculated from the t-plot. The task of detecting deviation from the standart isotherm is essentially one of comparing the shape of the isotherm under test with that of standart non-porous material by finding whether the two can be brought into coincidence by adjustment of the ordinate scales. Such test is provided by the t-plot. It is based on the t-curve, which is a plot of the standard isotherm with t, the statistical thickness of the film, given with the equation:

$$t = [\ 13.99 / (0.0340 - \log (P/P_o))\ ]^{0.5} \quad (4.3)$$

The isotherm under test is re-drawn as a t-plot (V vs t). The intercept on the adsorption axis of the extrapolated linear branch gives the micropore contribution and when converted to a liquid volume may be taken as equal to the micropore volume. If mesopores are present in addition to micropores, the plot will show an upward deviation at high relative pressures. The slope of the linear branch will then be proportional to the area of the mesopore walls together with the external surface.

The nitrogen adsorption isotherms have also been treated by the Dubinin-Astakhov method to obtain the limiting micropore volume, V_{lim}, exponential constant, n, and characteristic energy, E. The results obtained by these methods are shown in Table 4.4. Recalling from Eqn (2.15) Dubinin-Astakhov equation is:

$$W/W_o = \exp [- (A/E)^n] \quad (4.4)$$

where n is an empirical constant. The parameter E, characteristic free energy of adsorption, in the D-A equation is related to pore dimension. This relationship between E and pore size depends on the surface coverage (Chen and Yang, 1996). In the Henry's Law region, applied in this study, E is less strongly depends on the pore size and also adsorbate-adsorbent interactions. The E value for original NCW zeolite is very low (11.05 kJ/mol) with respect to acid treated forms. The formation of new pores accessible for nitrogen causes to increase the E values. According to Suziki (1990), the parameter n in the D-A equation may originally be considered to have integer values of 1, 2 and 3 corresponding to adsorption on the surface, in the micropores and ultramicropores respectively due to the losing of one, two or three degrees of freedom of the adsorbed molecules. Then it was realized that n is not necessarily an integer. Its value is about 1 for original natural zeolites. The parameter n achieves the value up to about 2 for acid treated zeolites. This proves that fine micropores took a part in the zeolite structure with having lower heterogeneity as acid treatment proceeds.

The n value in the D-A equation has been referred as the heterogeneity factor and it has been suggested that it is related to heterogeneity with respect to pore size distribution. For the adsorbents that have apparent micropore size distributions, the heterogeneity increases with decrease of the n value. For the pore size distributions of the zeolite samples, Horvath – Kawazoe (HK) method was used. In its original form, eqn:

$$\ln(p/p^{o}) = \frac{61.63}{(H - 0.64)}\left[\frac{1.895 \times 10^{-3}}{(H - 0.32)^{3}} - \frac{2.709 \times 10^{-7}}{(H - 0.32)^{9}} - 0.05014\right] \qquad (4.5)$$

where H is distance between the atom centers and expressed in nm.

The HK analysis was applied to nitrogen isotherms determined on molecular sieve adsorbents, the assumption being made that these adsorbents contained slit-shaped pores. The HK method is based on the general idea that the relative pressure required for the filling of micropores of a given size and shape is directly related to the adsorbent – adsorbate interaction energy.

Table 4.4. Micromeritics Data for the original and acid treated zeolites

	NCU	NCW	C1-6h	C3-6h	C5-6h	C10-6h	C3-3h	C10-3h	S1	S2	N1	N2	N5	P1
V_{mic}[a]	0. 0048	0. 005	0. 029	0. 064	0. 063	0. 047	0. 056	0 .047	0. 048	0. 055	0. 062	0. 068	0. 049	0. 04
$A_{Ext.Sur.}$[a]	5. 11	3. 08	6. 2	15. 2	25. 8	28. 7	17. 2	33	25. 3	33. 8	19. 9	22. 5	28. 5	6. 5
Langm.[b]	21	19	93	203	213	173	182	179	171	202	202	226	180	118
V_{lim}[c]	0. 0081	0. 01	0. 036	0. 072	0. 078	0. 059	0. 064	0. 073	0. 060	0. 079	0. 077	0. 082	0. 072	0. 043
n[c]	1.34	1.00	1.60	1.76	1.61	2.38	2.26	1.02	1.61	1.03	1.12	2.63	1.00	1.88
E[c]	15.85	11.05	19.31	28.37	21.63	21.39	20.98	22.76	28.76	26.75	35.63	25.42	26.72	25.23
V_{max}[d]	0.015	0.013	0.04	0.078	0.089	0.073	0.072	0.079	0.073	0.086	0.086	0.09	0.078	0.05
V_{lim}/V_{max}[e]	0.54	0.77	0.9	0.92	0.87	0.81	0.89	0.92	0.82	0.92	0.95	0.86	0.92	0.86

[a] Micropore volume (cm^3/g) and External Surface Area (m^2/g) respectively, from t-plot

[b] Langmuir surface area (m^2/g)

[c] V_{lim}, Limiting micropore volume (cm^3/g), n, exponential constant, and E, Characteristic Energy (kj /mol), from Dubinin – Astakhov (P/P_o= 0.0001-0.1)

[d] Maximum amount adsorbed at relative pressure (P/P_o) of 0.89

[e] Ratio of limiting micropore volume to maximum amount adsorbed at (P/P_o) of 0.89

The micropore or limiting volume of original zeolites (NCU and NCW) are almost the same and low (about 0.005 and 0.009 cm^3/g) while acid treated zeolites have higher volumes. The ionic radii of exchangeable cations, Ca^{2+}, Na^{+}, K^{2+}, Mg^{+} are 1.14, 1.16, 1.51 and 0.72 Å, respectively, and these cations occupy the considerable space in micropores of zeolites. In case of acid treated zeolites, the space occupied by either protons or hydroxyl group is negligible. Therefore, nitrogen was able to diffuse more easily and to be adsorbed more densely in acid treated zeolite cavities than in original zeolites, resulting in increased adsorption capacities. With acid treatments, the maximum nitrogen adsorption capacity ($P/P_o = 0.89$) of natural zeolite (0.015 cm^3/g) was increased to 0.089, 0.090, 0.086, and 0.050 cm^3/g for HCl, HNO_3, H_2SO_4 and H_3PO_4 treatments respectively. The high values calculated for the ratio of the limiting micropore volume to the maximum amount adsorbed shows that adsorption mostly took place in the zeolite crystals.

With HCl treatment for 6h, the amount of adsorption is increased with increasing concentration up to 5 M, (Si/Al = 8.4), but more increase in acid concentration caused to decrease the adsorption capacity. Similar behavior was observed during HNO_3 treatment; even the change in Si/Al ratio is small when compared to the HCl treatment. Nitrogen adsorption decreased with increasing HNO_3 concentration after 2 M HNO_3 (Si/Al = 6.18), and decreased with 5 M HNO_3 treatment. Acid treatment with other acids (H_2SO_4 and H_3PO_4) was not very effective on the Si/Al ratio and nitrogen adsorption. In the samples showing the decrease in the amount of adsorption, the plateau region disappears and the isotherm shape becoming clear to that of type II (Figures 4.16 - 4.18). This result suggests that acid treatment firstly makes zeolites ultramicroporous adsorbents in which the pores are narrow, and then supermicroporous adsorbents in which the pores are wide. Specific surface area of the original zeolite ($21 m^2/g$) increased up to 213 m^2/g with 5 M HCl, to 226 m^2/g with 2 M HNO_3, to 202 m^2/g with 2 M H_2SO_4, and to 118 m^2/g with 1.1 M H_3PO_4 treatments respectively (Table 4.4). When the results of 3 M HCl treated samples for 3 and 6 hours, C3-3h and C3-6h respectively, are compared, it is clear that, with the increased treatment time, nitrogen adsorption capacities increased slightly. The

changes in the external surface areas and micropore volumes of the HCl treated samples with respect to their Si/Al ratios are displayed in Figure 4.21.

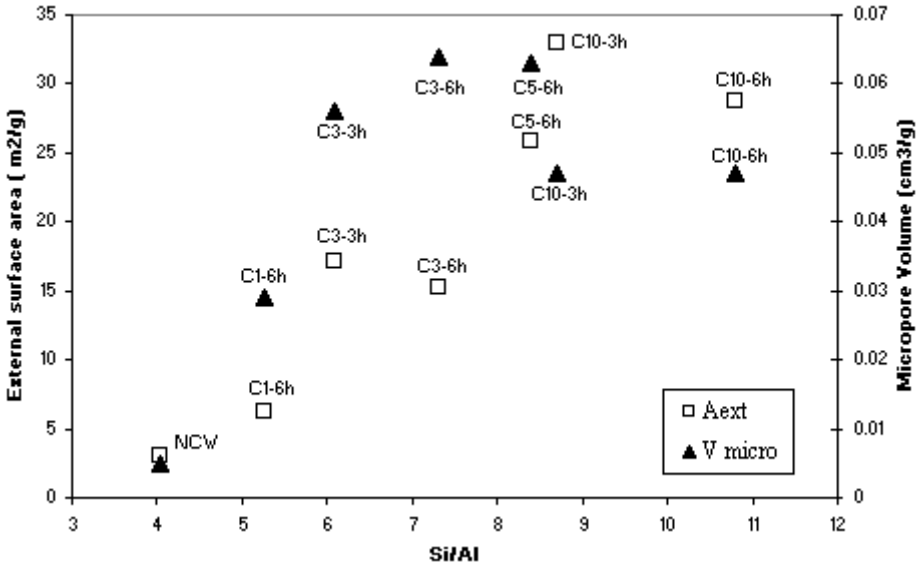

Figure 4.21. Micropore Volumes, V_{micro} , and External Surface Areas, A_{ext} , of the HCl treated zeolites vs Si/Al ratios (numbers in the sample code names shows the concentration of HCl used and the treatment time)

The micropore volume reached a maximum with C3-6h and C5-6h samples. Regarding this, it may be evaluated that with 3 M and 5 M HCl treatments, some of the cations in the channels of the crystals and the extraframework aluminas were removed from the structure, generating new pores accessible for nitrogen adsorption remaining the tetrahedral structure less attacked, confirmed by XRD analyses also. For the 10 M HCl treatments, the collapse of the pores are responsible for the decrease in the nitrogen capacities of the zeolites. Although nearly the same XRD patterns (same amorphization rates) were obtained with 1 M and 10 M HCl treatments (Figure 4.13), the inabilities of the aluminum complexes to migrate out of the structure in 1 M HCl treated sample act like pore-blockers, whereas in 10 M HCl treated sample these molecules were removed from the structure, but destroying newly generated pores. Therefore it is an expected result that 10 M HCl treatment resulted with a higher adsorption capacity than 1 M HCl treatment. Instead of a peak maxima for external surface areas, a continuously increase was observed (Figure 4.21). Increases in the external surface areas were caused by the dissolution of the silica units from the

framework due to the usage of high acid concentrations. This dissolution was probably initiated by lattice defects created by dealumination, which weakened the structure locally and finally resulted with the formation of mesopores in the crystal structure. These results were also supported by the literature (Giudici et al, 2000). Pore size distributions of the zeolites are given in Figures 4.22 through 4.26. Due to lack of data points below 5 Å, the micropore region of 5 – 20 Å are displayed. Wide distributions of the pores in the region was observed for the samples. With introducing acids to the zeolites, increased pore volumes were achieved, highest with HCl (6h) and HNO_3 treatments (Figures 4.22 and 4.24). 3h treatments resulted with more distributed micropore region, whereas with 6h treatments smaller pore diameters were more densely observed. H_2SO_4 and H_3PO_4 treatments displayed wide distribution of micropores but with smaller micropore volumes when compared with the other acid treatments (Figures 4.25 and 4.26).

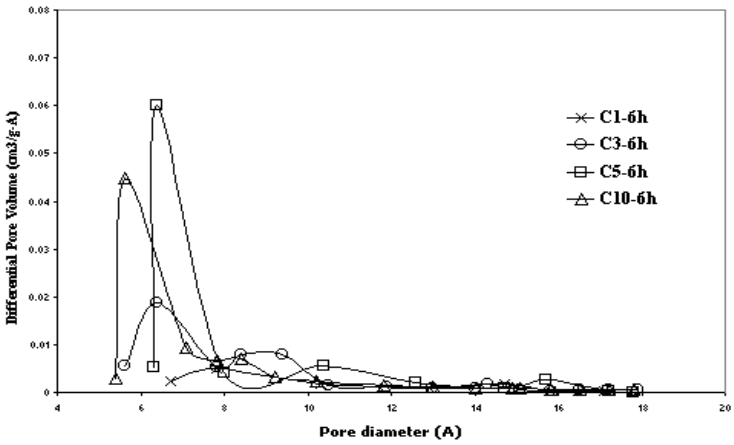

Figure 4.22. Pore size distributions of HCl (6h) treated zeolites

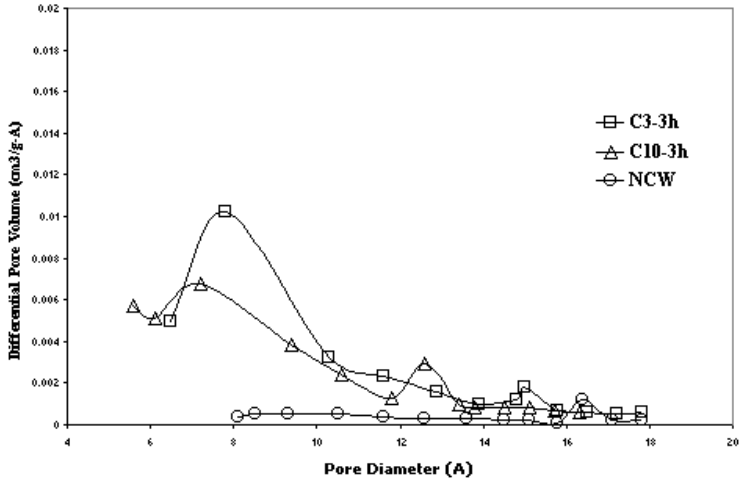

Figure 4.23. Pore size distributions of HCl (3h) treated zeolites and original zeolite

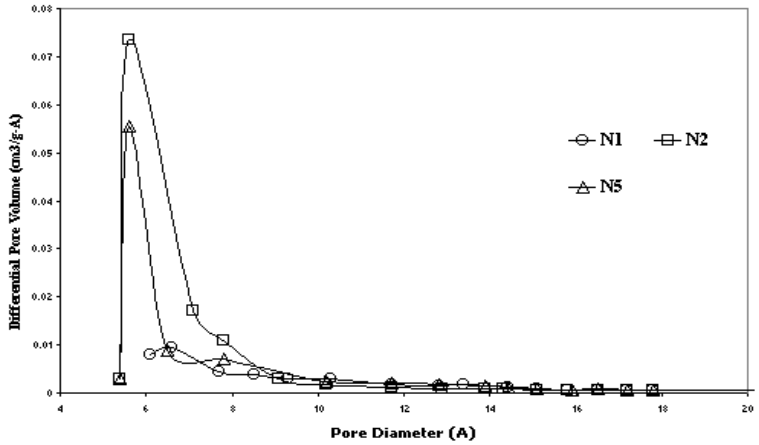

Figure 4.24. Pore size distributions of HNO_3 treated zeolites

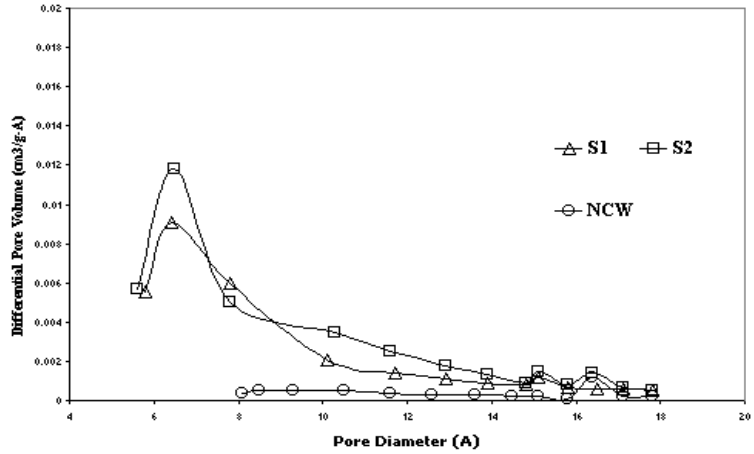

Figure 4.25. Pore size distributions of H_2SO_4 treated zeolites and original zeolite

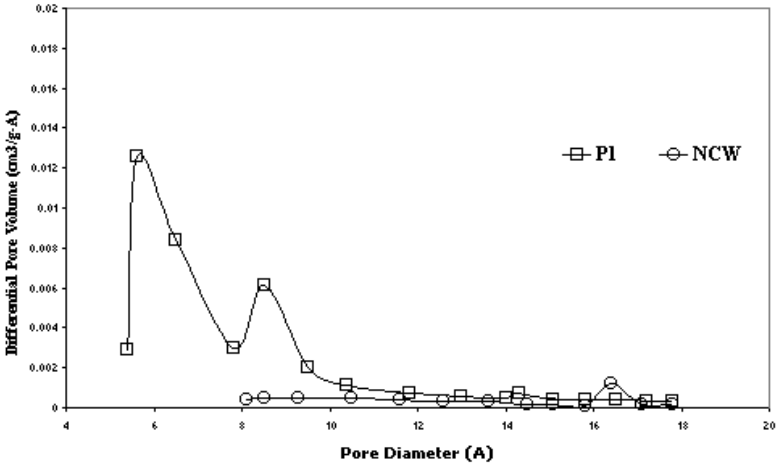

Figure 4.26. Pore size distributions of H_3PO_4 treated zeolite and original zeolite

4.5. Infrared Spectroscopy Analyses of the Original and Acid Treated Zeolites

Infrared spectroscopy has been used successfully for studying zeolite structure and properties (Goryainov et al, 1995). Asymmetrical stretching vibrations of internal tetrahedra linkages due to Si-O-Al bondings in the framework (1066 cm^{-1}), internal tetrahedra T-O bending (455cm^{-1}) and external tetrahedra double ring due to O-T-O bending (607cm^{-1}), the T-O asymmetric stretching vibration of free tetrahedra (1202-1212 cm^{-1}) and external tetrahedral linkage symmetric streching (795 cm^{-1}) are the characteristics for the clinoptilolite mineral. It turned out by comparison of spectral and structural features that the internal vibrations are largely structure insensitive, whereas the position of the bands due to vibrations of external linkages are often structure sensitive (Weitkamp and Puppe, 1999). Among the other bands, external tetrahedra double ring vibration was selected as the representative band for the clinoptilolite detection by referring the study of Goryainov et al (1995). The IR spectra of the original and the acid treated zeolites are given in Figures 4.27 - 4.31.

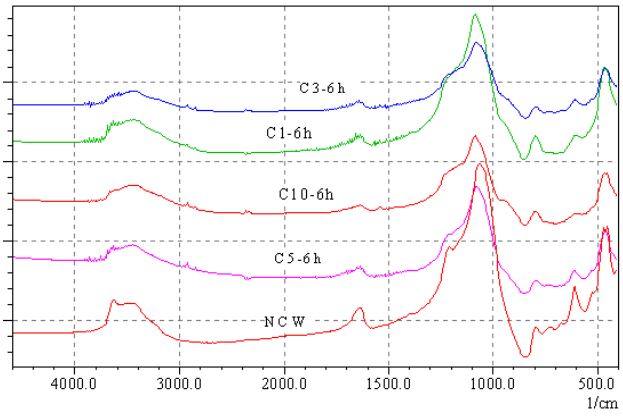

Figure 4.27. IR spectra of washed and HCl treated (6h) samples (absorbance in a.u. vs wavenumber)

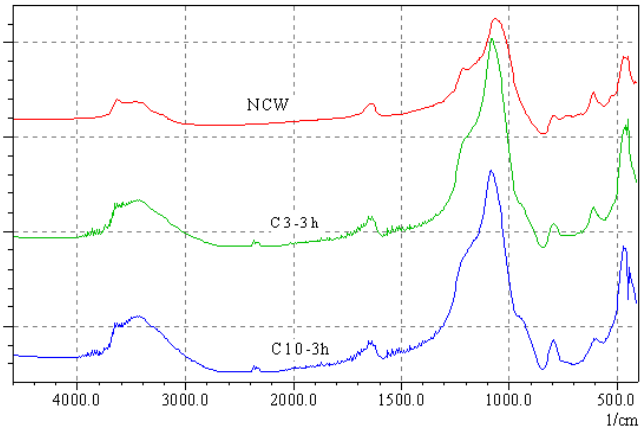

Figure 4.28. IR spectra of washed and HCl treated (3h) samples (absorbance in a.u. vs wavenumber)

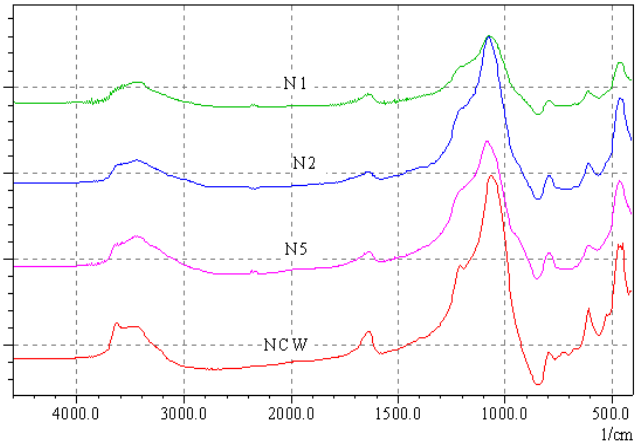

Figure 4.29. IR spectra of washed and HNO_3 treated samples (absorbance in a.u. vs wavenumber)

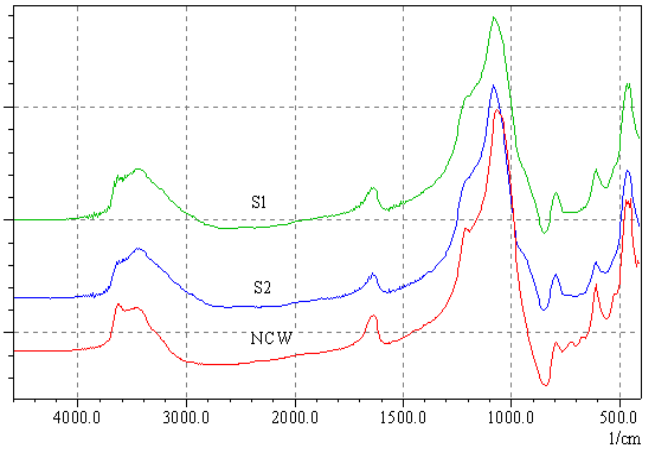

Figure 4.30. IR spectra of washed and H_2SO_4 treated samples (absorbance in a.u. vs wavenumber)

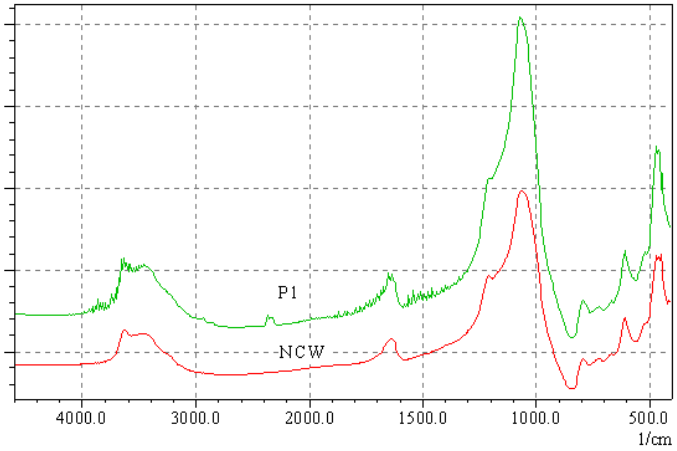

Figure 4.31. IR spectra of washed and H_3PO_4 treated sample (absorbance in a.u. vs wavenumber)

In Figure 4.32 wavelength shifts of the acid treated samples are displayed. According to Pozas et al (1996) and Doula et al (2002), the shift in the asymmetric O-T-O bending vibration to the higher wavenumbers could be caused by strong dealumination from the framework, because for highly siliceous zeolites, like ZSM-5, this band is located at around 1100 cm^{-1}. Increase in the concentrations of HNO_3 caused to shift the IR vibration of the zeolite structure to the higher wavenumbers confirming the Si/Al ratios, XRD and nitrogen adsorption results. Therefore it may be said that increase in the HNO_3 concentrations resulted in the removal of some of the framework aluminium as

well as the extraframework cations and caused to increase the adsorption capacities until the start of the crystal collapse with 5 M HNO_3 treatment. With the increase in the H_2SO_4 concentrations no shifts were observed meaning that there are no significant differences in the dealumination rates of those two zeolites. This was not surprising since the XRD results, Si/Al ratios (5.25 and 5.35) and the nitrogen adsorption capacities of those two zeolites (S1 and S2) showed great similarities. With the HCl treatment, IR band shifted to the lower wavenumbers for the treated samples up to 5 M HCl treatment and then 10 M HCl treatment caused to shift the band to the higher wavenumbers. These results are consistent with the Si/Al ratios, XRD patterns and nitrogen adsorption results of the HCl treated zeolites. IR strongest wavelength shifts of 1 M and 10 M HCl treated zeolites are due to the strong dealumination of the framework aluminas, which were also detected by the XRD analyses as the crystal collapses. 1.1 M H_3PO_4 treatment caused to shift the band slightly from 1060 cm^{-1} to 1070 cm^{-1} confirming the other characterization results, as no significant change in the zeolite structure had occurred after the treatment.

Peak intensity ratios (Figure 4.33 and 4.34) are given in order to see the relative change of the external tetrahedra double ring vibration, which is the representative band for clinoptilolite detection with respect to the other vibrations. It was observed that with increases in the HNO_3 and H_2SO_4 concentrations, peak intensity ratios decreased; indicating the loss of clinoptilolite content in the samples in consistency with the XRD results. With the HCl treatments, these ratios were found to be very low for 1 M and 10 M HCl treated samples confirming the XRD results. H_3PO_4 treatment resulted with similar peak intensity ratios with the NCW zeolite as expected.

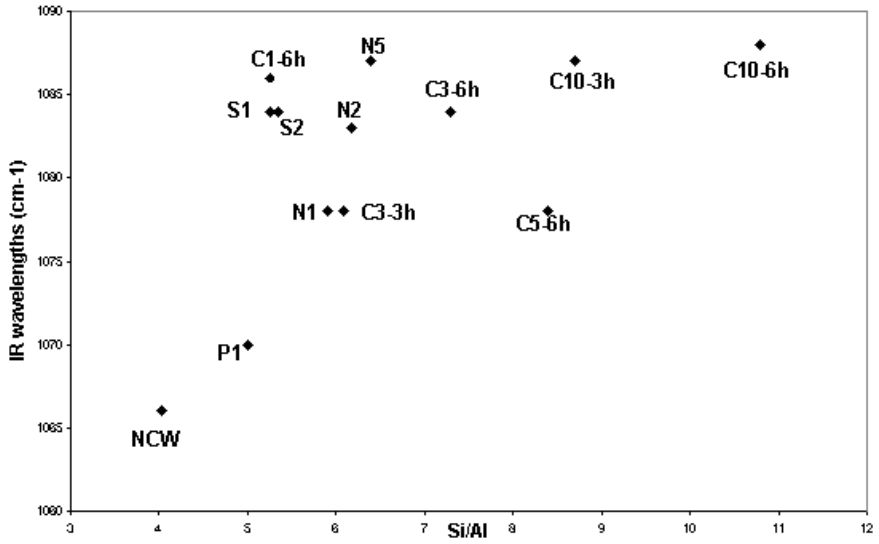

Figure 4.32. IR wavelength shifts of the internal asymmetrical stretching vibrations for all the samples vs Si/Al ratios

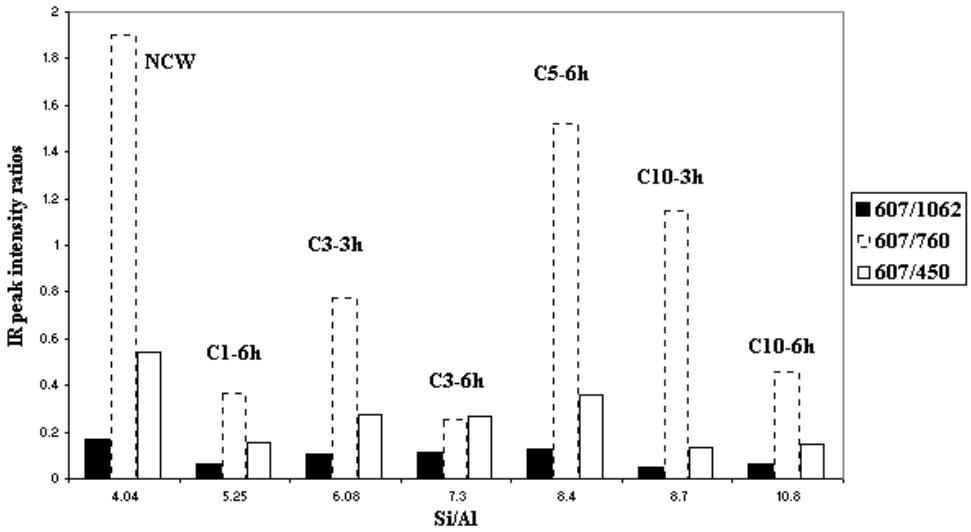

Figure 4.33. IR peak intensity ratios of washed original zeolite (NCW) and HCl treated zeolites vs Si/Al ratios

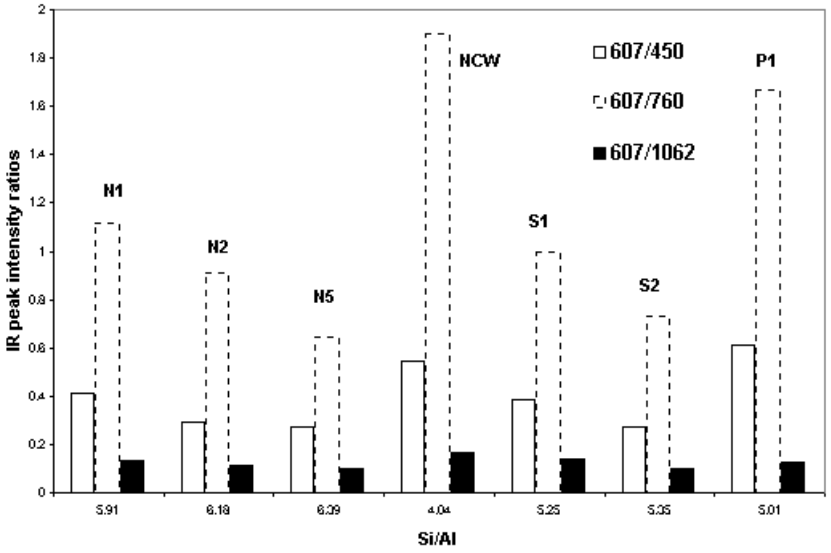

Figure 4.34. IR peak intensity ratios of washed original zeolite (NCW) and HNO_3, H_2SO_4 and H_3PO_4 treated samples with their Si/Al ratios

4.6. Scanning Electron Microscopy Analysis of the Acid Treated Zeolites

In Figures 4.35 - 4.37, SEM microphotographs of 1 M HCl (C1-6h), 10 M HCl (C10-6h) and 5 M HNO_3 (N5) treated zeolites are displayed in order to show the collapses of the crystals and amorphizations due to the acid treatments, confirming the XRD results.

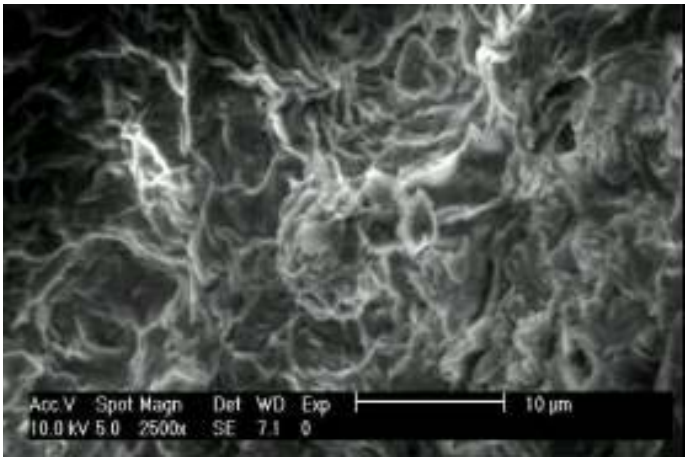

Figure 4.35. SEM microphotograph of 1 M HCl treated zeolite

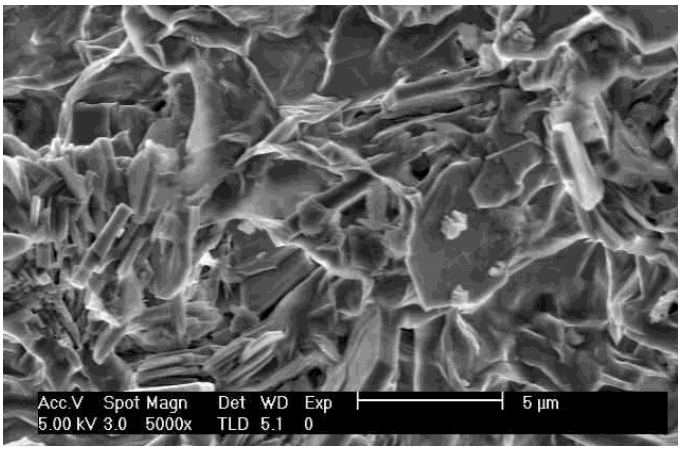

Figure 4.36. SEM microphotograph of 10 M HCl (3h) treated zeolite

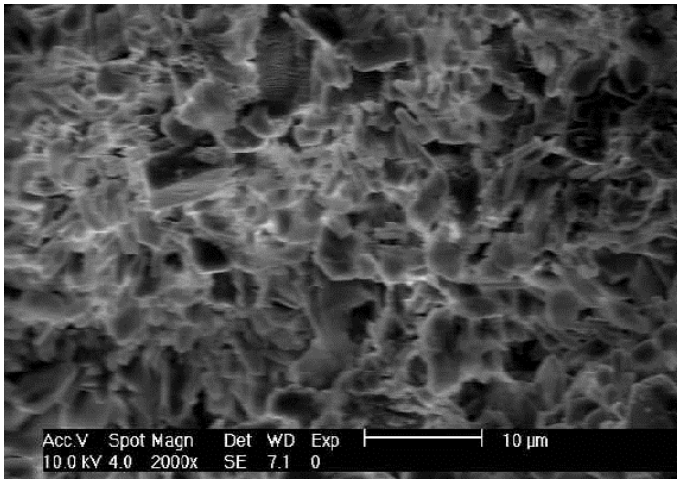

Figure 4.37. SEM microphotograph of 5 M HNO_3 treated zeolite

4.7. Thermal Behaviour of the Acid Treated Zeolites

Thermoanalytical techniques have been found to yield information on the mechanism as well as the thermal behaviour of zeolite. In this study, an attempt was made to investigate the thermal properties of sample with different chemical composition having the same structural features, using thermoanalytical techniques such as DTA and TG / DTG. As seen from the representative DTA figures (Figures 4.38- 4.40), between about 400 – 1000 ^{o}C one endotherm and one exotherm was observed for the samples; The endothermic peak is due to the decompositon of the other phases (zeolitic and unzeolitic) in the zeolite framework, while exothermic peak obtained at about 950 ^{o}C is attributed to the collapse of the zeolite lattice depending on the removal of zeolitic water and sometimes at much higher temperatures recrystallization to a new phase (Riberio et al, 1984). In our case the endotherm in the low temperature region with a maxima at around 80 ^{o}C and finishes at around 200 ^{o}C is typical for zeolites and caused by the evolution of water and possibly other volatile substances in the zeolite cavities. The exothermic peak, around 200 – 400 ^{o}C is not common for the zeolites and shows some exothermic reaction happening at that temperature, and may probably be caused by recrystallization in the clinoptilolite structure. This phenomena is still under investigation.

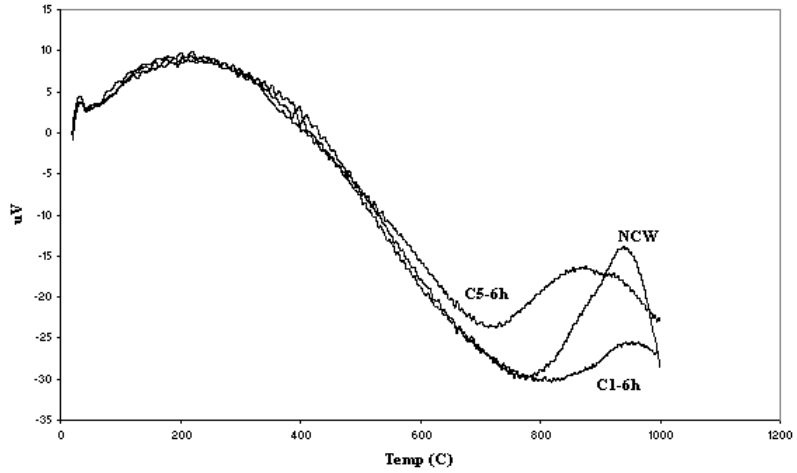

Figure 4.38. DTA curves of original washed (NCW) and 1 M and 5 M HCl treated zeolites

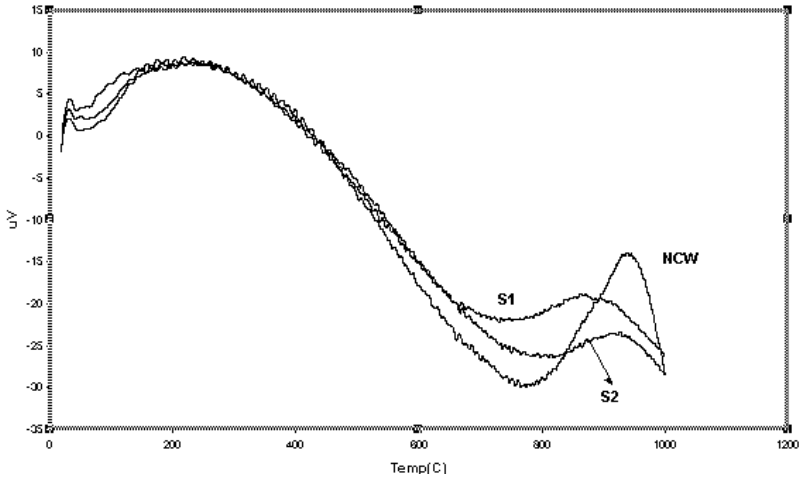

Figure 4.39. DTA curves of original washed (NCW) and H_2SO_4 treated zeolites

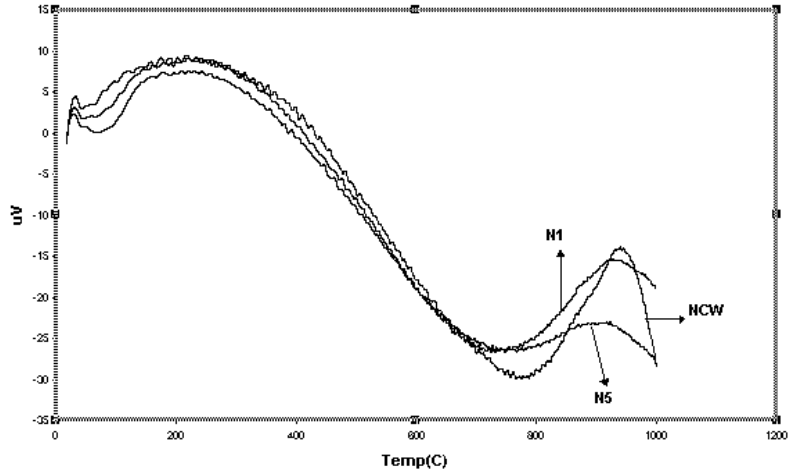

Figure 4.40. DTA curves of original washed (NCW) and 1 M and 5 M HNO_3 treated zeolites

TGA and derivative TGA (DTGA) curves of acid treated zeolites and original zeolite (NCW) are shown in Figures 4.41 - 4.50.

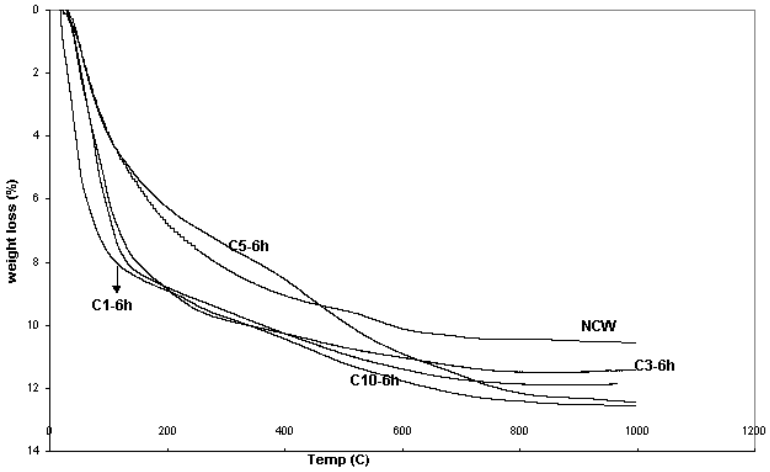

Figure 4.41. TGA curves of washed original (NCW) and HCl treated (6h) samples

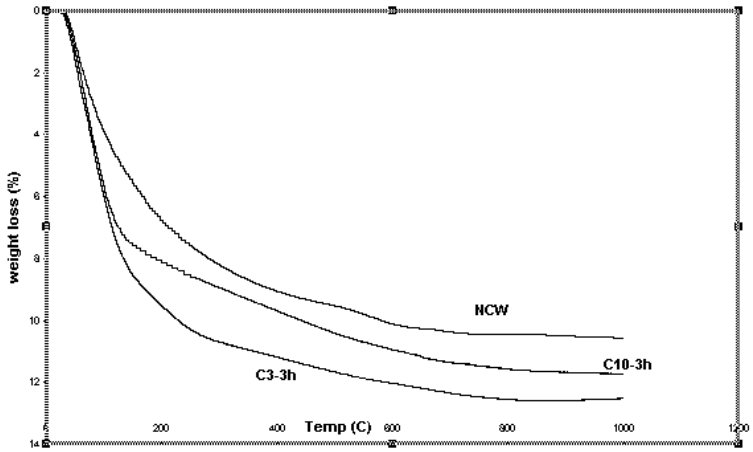

Figure 4.42. TGA curves of washed original (NCW) and HCl treated (3h) samples

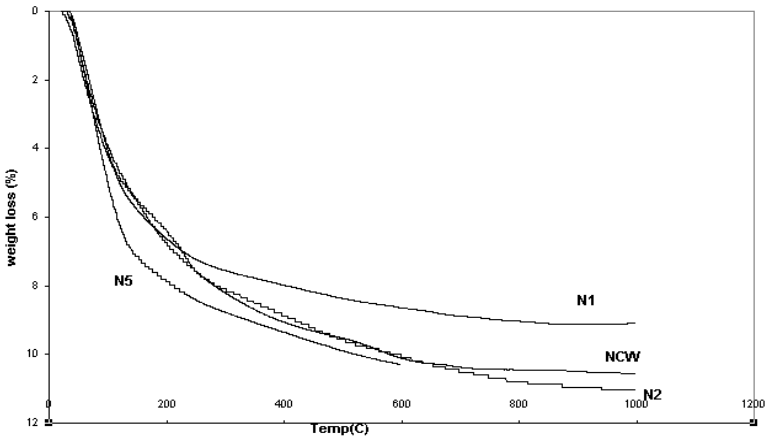

Figure 4.43. TGA curves of washed original (NCW) and HNO_3 treated samples

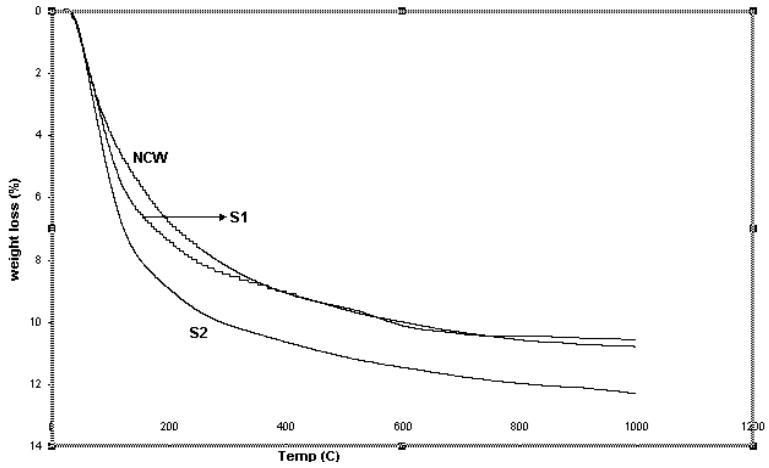

Figure 4.44. TGA curves of washed original (NCW) and H_2SO_4 treated samples

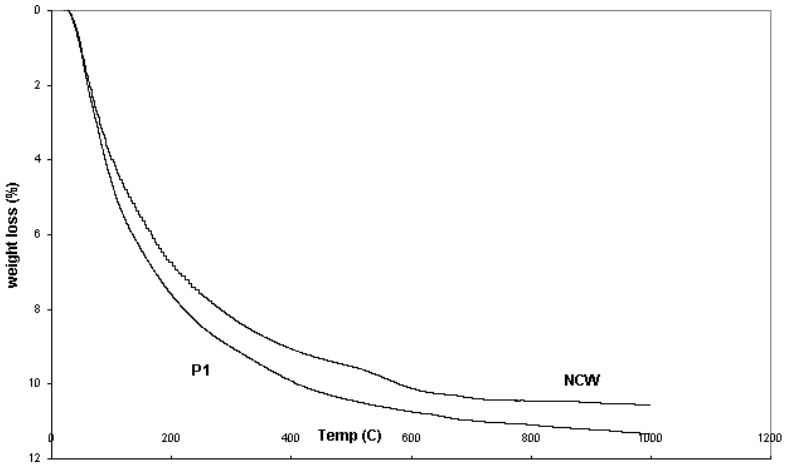

Figure 4.45. TGA curves of washed original (NCW) and H_3PO_4 treated samples

From the derivative TGA curves below, two peak minimums were achieved below 80 ^oC indicating the desorption of water from the surface and the start of losing the so-called loosely held water. Then the trend of the derivative TGA curves is same up to about 200-300 ^oC depending on the samples and then starts to be plateau-like, but still indicating water loss after 400 ^oC.

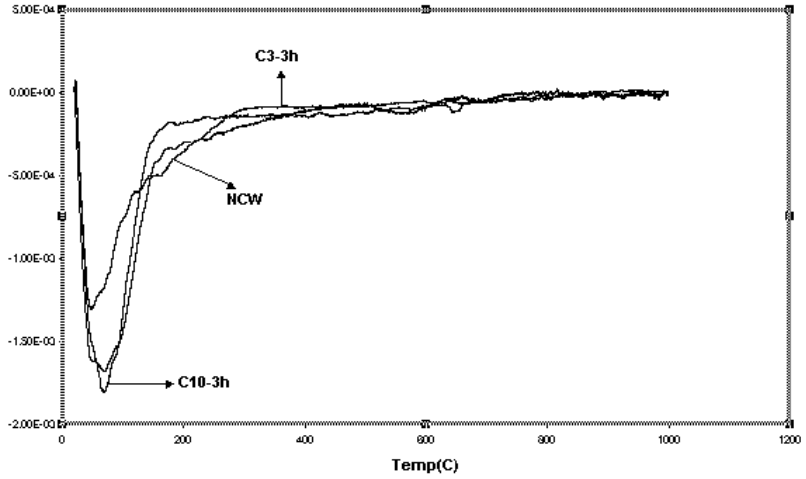

Figure 4.46. Derivative TGA curves of HCl treated (3h) samples

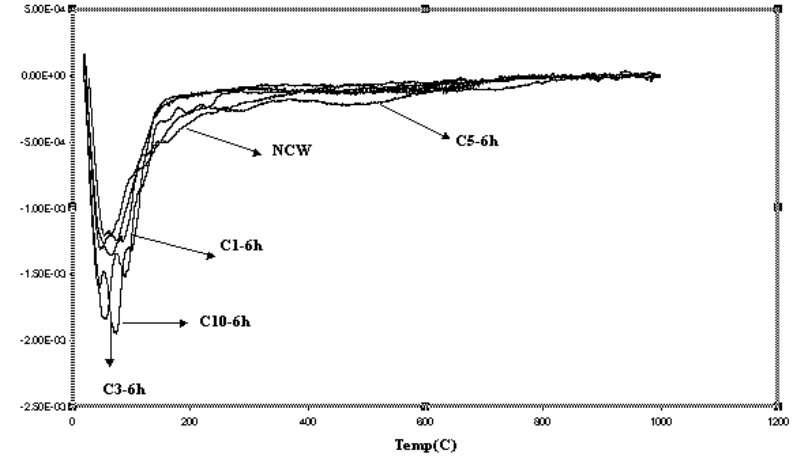

Figure 4.47. Derivative TGA curves of washed and HCl treated (6h) samples

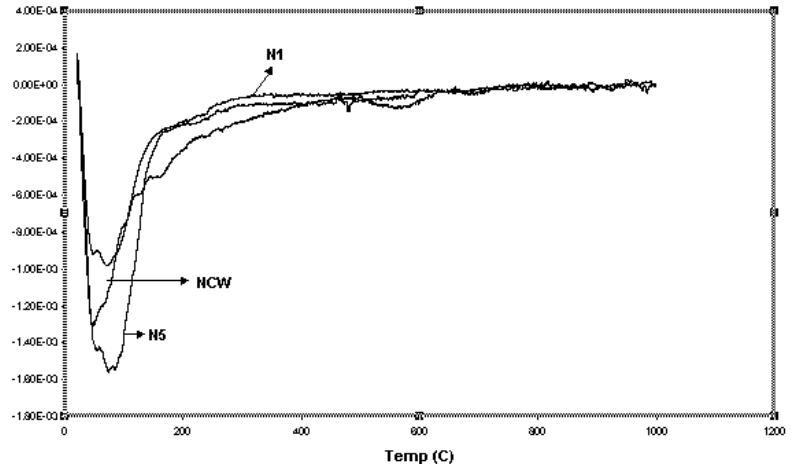

Figure 4.48. Derivative TGA curves of washed, 1M and 5 M HNO_3 treated samples

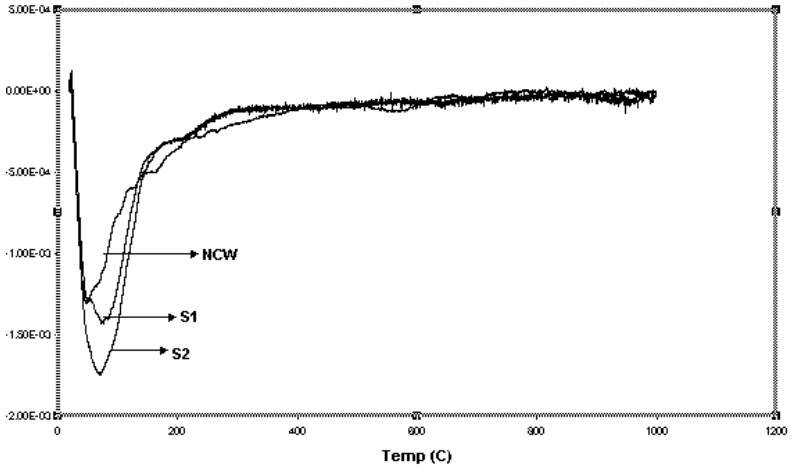

Figure 4.49. Derivative TGA curves of washed and H_2SO_4 treated samples

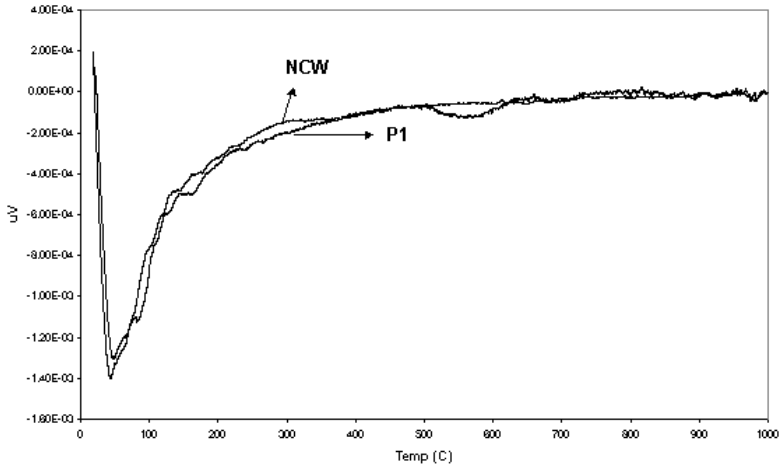

Figure 4.50. Derivative TGA curves of washed and H_3PO_4 treated samples

The weight losses of samples in percentages as they were heated up to ~ 1000 ^oC were determined from the TGA curves and are represented in Table 4.5. Three temperature regions are distinguished.

Table 4.5. Weight loss percent of total weight loss of samples

Sample name	(30-200 ^{o}C), %	(200-400 ^{o}C), %	(400-1000 ^{o}C), %	Total weight loss, %
NCW	64	22	14	10.56
C1-6h*	68.9 ± 1.5	12.9± 0.5	18.2 ± 1	10.56 ± 2
C3-6h	78	12	10	11.2
C5-6h*	52.4 ± 1	18.9 ± 0.5	28.7 ± 2	12.23 ± 0.2
C10-6h	74	12	14	11.6
C3-3h	77	12.4	10.6	12.3
C10-3h	70	14	16	11.6
S1	68.3	15.9	15.8	10.78
S2*	72 ± 0.5	13.5 ± 0.5	14.5 ± 1	12.21 ± 0.07
N1	72.9	14.9	12.2	9.08
N2*	57.8 ± 0.25	22.6 ± 0.2	19.6 ± 0.2	11.04
N5	76.8	14.2	9	10.28
P1*	67.5 ± 0.3	19.4 ± 1	13.1 ± 0.5	11.21 ± 0.1

*two TGA results were taken

Total weight loss of the zeolites showed an increase with the increase in the Si/Al ratios, then decreased with the 10 M HCl and 5 M HNO_3 treatments, confirming the pre-discussed characterization results, showing the decrease in the pore volumes with these acids. Weight loss percents of the samples between 200 and 400 ^{o}C is lower (12-22 %) than those up to 200 ^{o}C. It is seen that samples continue to loose water after 400 ^{o}C. Alberti and Vezzalini in 1978 speculated that all zeolites exhibiting water losses at temperatures > 400 ^{o}C contain hydroxide ions that probably form through reaction of intracrystalline H_2O molecules with the tetrahedral framework (Bish, 1995). Exothermic reaction happening at elevated temperatures may be because of the intracrystalline H_2O molecules.

On the other hand Van Reeuwijk classified water in zeolites into three categories based on calorimetrically measured heats of dehydration: loosely held water, zeolitic water, and crystal water with denser zeolites containing primarily crystal water and more open zeolites containing zeolitic water (Bish, 1995). Knowlton et al. (1981) observed the existence of three-bound water in zeolite structure from the derivative TGA (DTGA) curves, which are surface water, loosely bound water and tightly bound water. Dehydration at low temperature (up to minimum on DTGA), about < 80 ^{o}C represent desorption of water from the surface of the grains in the powder sample. From this minimum temperature up to 200 ^{o}C, the loosely bound water is desorbed. The tightly bound water, and also called the zeolitic water is desorbed in the temperature range of 200-700 ^{o}C according to Knowlton et al. (1981). According to Bish (1995), distinct types of water such as loosely bound or tightly bound zeolitic water do not exist. Rather, water is bound, primarily to extra-framework with a continuum of energies, giving rise to a pseudocontinuous loss of water accompanied by a dynamic interaction between remaining H_2O molecules, extraframework cations, and the tetrahedral framework. These interactions in the channels of zeolites give rise to dehydration behaviour that is very dependent on the nature of the extraframework cations in addition to temperature and water vapor pressure. As some H_2O molecules evolve at lower temperatures, remaining H_2O molecules are attracted more strongly to extraframework cations. The nature of zeolite dehydration (and the total amount of H_2O) is strongly dependent on the hydration energies of the extraframework cations, such as Ca^{2+}, contain significantly more H_2O than those containing low-hydration-energy cations, such as K^{+}, and those with high-hydration energy cations also generally retain their H_2O to higher temperatures (Bish, 1995). Acid treated samples have undoubtfully less cation content in their structures than the original zeolite (NCW) due to the removal of cations, this may help to explain the general trend which is, NCW zeolite is more unlikely to release water than the acid treated zeolites.

4.8. Heat Capacity Measurements of the Zeolites

Heat capacities at 26 ^{o}C of the original and the acid treated samples are shown in Table 4.6. As the acid concentrations increased, the heat capacities also increased for the HCl and H_2SO_4 treated samples, while for the HNO_3 treated samples, they decreased.

Table 4.6. Heat capacities of the original and the acid treated samples

Sample name	C_p^*(J/K.gr) at 26^{o}C
NCU	1.1126
NCW	1.1167
S1	1.1395
S2	1.2092
C1-6h	1.0209
C5-6h	1.2501
N1	1.1305
N5	1.0775

* heat capacity

The as-received (NCU) and washed (NCW) original zeolites have low heat capacities in comparison with its acid acid treated forms except N5 and C1-6h zeolite. Heat capacity is governed by structural changes (electrostatic, ionic radius, mass, volume and nature of interaction) and this increase can be explained by decrease in stearic and electrostatic effects but increase in pore volume with extent of acid treatment.

NCU zeolite has lower heat capacity than NCW zeolite depending on the impurities in zeolitic tuff. The measured C_p for NCW is in accordance with literary data for the clinoptilolite depending on its compositions:

C_p= 1,0890 J/gK ($Na_{0,56}$ $K_{0,98}$ $Ca_{1,50}$ $Mg_{1,.23}$ $Al_{6,7}$ $Fe_{0,3}$ Si_{29} O_{72} 22 H_2O) (Hemingway and Robie, 1984) and C_p =1,1288 kJ / kg K ($Sr_{0,036}$ $Mg_{0,124}$ $Ca_{0,76}$ $Mn_{0,002}$ $Ba_{0,062}$ $K_{0,543}$ $Na_{0,954}$ $Al_{3,457}$ $Fe_{0,017}$ $Si_{14,533}$ $O_{36,00}$ 10 H_2O) (Johnson et al , 1991).

CONCLUSIONS

Natural zeolitic tuff from Gördes, Fındıcak region (Manisa, Turkey), characterized as clinoptilolite with some quartz and cristoballite as crystalline impurities, was modified with acid solutions (HCl, H_2SO_4, HNO_3, and H_3PO_4) at 60 ^oC for 6 and 3 hours to improve its nitrogen adsorption properties. In the acid treatments applied in this study, not only the acid concentrations but also the nature of the acid and the duration of treatment were effective on modification of natural zeolite structure.

Acid treatment of the natural zeolites improved its nitrogen adsorption via the mechanism of decationization and dealumination also by dissolution of any amorphous silica, blocking the channels of clinoptilolite structure.

The bulk Si/Al ratios are increased; from 4.04 to 10.8 with HCl, from 4.04 to 6.39 with HNO_3, from 4.04 to 5.35 with H_2SO_4, and from 4.04 to 5.01 with H_3PO_4 treatments, with increasing the concentration of acids.

Nitrogen adsorption uptake of the HCl treated zeolites started to decrease after 5 M HCl treatment (Si/Al = 8.4) due to the collapse of the crystal structure that was detected by XRD analysis and SEM microphotographs, whereas this uptake decrease was observed after 2 M HNO_3 treatment (Si/Al = 6.18) showing that these two acids attacked very strongly to the structure. H_2SO_4 and H_3PO_4 treatments were found to be not very effective on Si/Al ratios and nitrogen capacities.

HCl and HNO_3 were the most effective acids on improvement the micropore structure of natural zeolites. Increase in the external surface areas from 5 to 33 m^2/g were observed with increasing the acid concentrations due to the formation of the mesopore system. FTIR results were also complementary to the above conclusions, declaring that the decrease in the framework alumina compositions and the clinoptilolite contents, showing the crystallinity losses of the samples with the acid treatments. Among the acid treated zeolites, the treated zeolites with 5 M HCl and 2 M HNO_3 have the the highest micropore volumes (0.063 and 0.068 cm^3/g), limiting micropore volumes (0.078 and 0.082 cm^3/g), and Langmuir surface areas (213 and 226 m^2/g) respectively.

According to the above results, it may be concluded that, these treated zeolites can be used as adsorbents in adsorption processes based on mainly nitrogen adsorption.

REFERENCES

- Abusafa, A., Yücel, H., " Removal of ^{137}Cs from aqueous solutions using different cationic forms of a natural zeolite: clinoptilolite ", Separation and Purification Technology 28 (2002), 103-116.
- Ackley, M.W., Yang, R.T., "Adsorption Characteristics of High-Exchange Clinoptilolites", Ind. Eng. Chem. Res. 1991, 30, 2523-2530.
- Adamson, A.W., Physical Chemistry of Surfaces, John Wiley and Sons Inc, 1990.
- Armbruster, T., " Clinoptilolite-heulandite applications and basic research" in Studies in Surface Science and Catalysis 135. Zeolites and Mesoporous Materials at the Dawn of the 21th Century. Galarnau, A., Renzo, F.D., Faujula, F. and Vedrine, J. (Editors), 2001. Elsvier Science B.V.
- Armenta, A.A., Ramirez, G.H., Loyola, E.F., Castaneda, A.U., Gonzales, R.S., Munoz, C.T., Lopez, A.J., Castellon, E.R., "Adsorption Kinetics of CO_2, O_2, N_2, and CH_4 in Cation-Exchanged Clinoptilolite", J. Phys. Chem. 2001, 105, 1313-1319.
- Armenta, G.A, and Jimenez, L.D., " Characterization of the porous structure of two naturally occurring materials through N_2 – adsorption (77K) and gas chromatographic methods", Colloids and Surfaces, 176 (2001) 245-252.
- Bish, D.L., "Thermal Behavior of Natural Zeolites", Natural Zeolites, D.W. Ming and F.A. Mumpton, eds, 1995, pp 259-269.
- Chang, R., Chemistry, Mc Graw-Hill, 1994.
- Chen, S.G., Yang, R.T., " Theoretical Investigations of Relationships Between Characteristic Energy and Pore Size for Adsorption in Micropores ", J. Col. and Interface Sciences, 1996, 177, 298-306.
- Doula, M., Ioannou, A., Dimirkou, A., "Copper Adsorption and Si, Al, Ca, Mg, and Na Release from Clinoptilolite", Journal of Colloid and Interface Science 245, 237-250 (2002).
- Drebushchak, V.A., Naumov, V.N., Nogteva, V.V., Belitsky, I.A. and Paukov, I.E. (2000), " Low-temperature heat capacity of heulandite: comparison with clinoptilolite", Thermochimica Acta, 348, 33-40.

- Esenli, F., " Gördes Neojen Havzasının Asitik Tüflerinde Zeolitleşme (Höylandit-Klinoptilolit Tip) ile Meydana Gelen Kimyasal Değişimler ", Türkiye Jeoloji Bülteni, C. 36, 37-44, Ağustos 1993.
- Ghobarkar, H., Schaf, O., and Guth, U., " Zeolites – from kitchen to space ", Prog. Solid St. Chem. Vol. 27, pp. 29-73, 1999.
- Giudici, R., Kouwenhoven, H.W., Prins, R., "Comparison of nitric and oxalic acid in the dealumination of mordenite", Applied Catalysis, 203 (2000) 101-110.
- Gola, A., Rebours, B., Milazzo, E., Lynch, J., Benazzi, E., Lacombe, S., Delevoye, L., Fernandez, C., " Effect of leaching agent in the dealumination of stabilized Y zeolites ", Microporous and Mesoporous Materials 40 (2000) 73-83.
- Goryainov, S.V., Stolpovskaya, V.N., Likhacheva, A.Y., Belitsky, I.A., and Fursenko, B.A., " Determination of Clinoptilolite and Heulandite in Tuffaceous Deposits by Infrared Spectroscopy", Natural Zeolites 93: Occurrence, Properties, Use, Ming, D.W. and Mumpton, F.A., 1995, pp 245-255.
- Gregg, S.J., Sing, K.S.W., Adsorption, Surface Area and Porosity, Academic Press, 1982.
- Helminen, J., Helenius, J., Paatero, E., " Comparison of Sorbents and Isotherm Models for NH_3-Gas Separation by Adsorption ", AIChe Journal, August 2000 Vol.46, No.8.
- Hemingway. B.S., and Robie, R.A., " Thermodynamics properties of zeolites: Low temperature heat capacities and thermodynamic functions of philipsite and clinoptilolite. Estimates of the thermodynamical properties of zeolitic water at low temperature", American Mineralogist, 1984, 69, 692-700.
- Hong, Y., Fripiat, J.J., " Microporous characteristics of H-Y, H-ZSM-5 and H-mordenite dealuminated by calcination ", Microporous Materials 4 (1995) 323-334.
- Huesca, R.H., Diaz, L., Armenta, G.A., "Adsorption equilibria and kinetics of CO_2, CH_4 and N_2 in natural zeolites", Separation and Purification Technology 15 (1999) 163-173.
- Iznaga, I.R., Gomez, A., Fuentes, G.R., Aguilar, A.B., Ballan, J.S., " Natural clinoptilolite as an exchanger of Ni^{2+} and NH_4^+ ions under hydrothermal conditions and high ammonia concentration ", Microporous and Mesoporous Materials 53 (2002) 71-80.

- Johnson, G.K., Tasker, I.R., Jurgens, R., and O'Hare, P.A.G., " Thermodynamic studies of zeolites: Clinoptilolite", Journal of Chemical Thermodynamics, 23, 475-484, 1991.
- Knowlton, G.D., White, T.R., McKague, H.L., " Thermal Study of Types of Water Associated With Clinoptilolite ", Clays and Clay Minerals, Vol. 29, No.5, 403-411, 1981.
- Malherbe, R.R., " Applications of Natural Zeolites in Pollution Abatement and Industry ", Handbook of Surfaces and Interfaces of Materials, edited by H.S. Nalwa, Volume 5: Biomolecules, Biointerfaces and Applications, 2001, 495-520.
- Malherbe, R.R., " Complementary approach to the volume filling theory of adsorption in zeolites ", Microporous and Mesoporous Materials 41 (2000) 227-240.
- Mumpton, F.A., " Clinoptilolite Redefined ", The American Mineralogist Vol 45, March-April, 1960.
- Notario, J.S., Garcia, J.E., Caceres, J.M., Arteaga, I.J., Gonzales, M.M., " Characterization of natural phillipsite modified with orthophosphoric acid ", Applied Clay Science 10 (1995), 209-217.
- Pozas, C., Kolodziejski, W., Malherbe, R.R., " Modification of clinoptilolite by leaching with orthophosphoric acid ", Microporous Materials 5 (1996) 325-331.
- Rege, S.U., Yang, R.T., Buzanowski, M.A., "Sorbents for air prepurification in air separation", Chemical Engineering Science 55 (2000) 4827-4838.
- Riberio, F.R., Rodrigues, A.E., Rollmann, L.D., Naccache, C., Zeolites: Science and Technology, Martinus Nijhoff Publishers, 1984.
- Rouquerol, F., Rouquerol, J., Sing, K., Adsorption by Powders and Porous Solids: Principles, Methodology and Applications, Academic Press, San Diego, 1999.
- Suzuki, M., Adsorption Engineering, Elsevier, 1990.
- Talu, O., Li, J., Kumar, R., Mathias, P.M., Moyer, J.D., Schork, J.M., " Measurement and Analysis of oxygen/nitrogen/ 5A-zeolite adsorption equilibria for air deparation ", Gas. Sep. Purif. Vol. 10, No.3, pp 149-159, 1996.
- Triebe, R.W., Tezel, F.H., "Adsorption of Nitrogen and Carbon Monoxide on Clinoptilolite: Determination and Prediction of Pure and Binary Isotherms", The Canadian Journal of Chemical Engineering, Volume 73, October, 1995.
- TSE, UDK 662.6: 543, 1984.

- Tsitsishvili G.V., Andronikashvili, T.G., Kirov, G.N., Filizova, L.D., Natural Zeolites, Ellis Horwood, New York, 1992.
- Vansant, E.F., Cool, P., " Chemical modifications of oxide surfaces ", Colloids and Surfaces, 179 (2001) 145-150.
- Weitkamp, J., Puppe, L., Catalysis and Zeolites, Verlag Berlin Heidelberg, 1999.
- Yaşyerli, S., Ar, I., Doğu, G., Doğu, T., " Removal of hydrogen sulfide by clinoptilolite in a fixed bed adsorber", Chemical Engineering and Processing 00 (2002) 1-8.
- Zhao, D., Cleare, K, Oliver, C., Ingram, C., Cook, D., Szostak, R., Kevan, L., " Characteristics of the Synthetic Heulandite-Clinoptilolite Family of Zeolites", Microporous and Mesoporous Materials, 21, 1998, pp. 371-379.